REPORT DOCUMENTATION PAGE

Form Approved
OMB No. 0704-0188

1. AGENCY USE ONLY (Leave Blank)	2. REPORT DATE	3. REPORT TYPE AND DATES COVERED
	AUG 92	Final

4. TITLE AND SUBTITLE
THE ROLE OF ENTANGLEMENTS IN THE SWELLING OF POLY(DIMETHYLSILOXANE) NETWORKS

5. FUNDING NUMBERS

6. AUTHOR(S)
SHAWN P. MALONE

7. PERFORMING ORGANIZATION NAME(S) AND ADDRESS(ES)
Cornell University
Ithaca, NY 14853

8. PERFORMING ORGANIZATION REPORT NUMBER

9. SPONSORING/MONITORING AGENCY NAME(S) AND ADDRESS(ES)

10. SPONSORING/MONITORING AGENCY REPORT NUMBER

11. SUPPLEMENTARY NOTES

12a. DISTRIBUTION/AVAILABILITY STATEMENT

This document has been approved for public release and sale; its distribution is unlimited.

12b. DISTRIBUTION CODE

13. ABSTRACT (Maximum 200 words)

The swelling of "model" and "imperfect" poly(dimethylsiloxane) networks in solvents and polymer chains were studied to see how the role of entanglements affect the predictions of the Flory-Rehner swelling model. The equilibrium elastic moduli, G_e, of the networks were found to be greater than the values predicted from the affine and phantom network theories. The imperfect networks gave values of G_e which dropped sharply from the constant plateau of model networks as more pendant chains were added. The results illustrate the entanglement contribution to the elastic modulus. When the entanglements were experimentally accounted for by using the experimentally measured elastic modulus, then the Flory-Rehner model coupled with the phantom network assumption adequately predicts the swelling results over a wide range of swelling extents.

14. SUBJECT TERMS
poly(dimethylsiloxane), synthesis, networks, entanglements, Flory-Rehner, interaction parameter, equilibrium swelling

15. NUMBER OF PAGES
121

16. PRICE CODE

17. SECURITY CLASSIFICATION OF REPORT	18. SECURITY CLASSIFICATION OF THIS PAGE	19. SECURITY CLASSIFICATION OF ABSTRACT	20. LIMITATION OF ABSTRACT
UNCLASSIFIED	UNCLASSIFIED	UNCLASSIFIED	

THE ROLE OF ENTANGLEMENTS IN THE SWELLING OF POLY(DIMETHYLSILOXANE) NETWORKS

A Thesis

Presented to the Faculty of the Graduate School

of Cornell University

in Partial Fulfillment of the Requirements for the Degree of

Master of Science

by

Shawn P. Malone

August 1992

ABSTRACT

The swelling of "model" and "imperfect" polydimethylsiloxane (PDMS) networks in solvents and polymer chains were studied to see how the role of entanglements affects the predictions of the Flory-Rehner swelling model.

The model networks were prepared by endlinking difunctional PDMS (B_2) with a given amount of tetrafunctional crosslinker (A_4) to obtain networks with a minimum amount of elastically ineffective chains. The imperfect networks were prepared by endlinking mixtures of monofunctional PDMS (B_1), B_2, and A_4 to obtain networks containing pendant chains and branched structures.

The equilibrium elastic moduli, G_e, of the networks were determined from dynamic mechanical experiments and were found to be greater than the values predicted from the affine and phantom network theories when using a branching model of nonlinear polymerization (Macosko-Miller model) to characterize the networks. The values of G_e for the model networks showed no dependence on ν, the calculated moles of elastic chains per unit volume for the range $6 < \nu < 30$ mol/m^3. For the networks with $\nu > 50$ mol/m^3, their moduli showed clearly a linear dependence on ν. The imperfect networks gave values of G_e which dropped sharply from the constant plateau value of model networks as more pendant chains were added. Imperfect networks prepared from high molecular weight B_2 with an equivalent amount of pendant chains (B_1) added as imperfect networks prepared from low molecular weight B_2 gave lower values of G_e. The results illustrate the entanglement contribution to the elastic modulus and

indicate that more trapped entanglements are released in the former than in the latter.

The extents of swelling at equilibrium of the networks in toluene and benzene were determined. The model networks swelled less than predicted by the affine and phantom models and less than imperfect networks with the same value of ν. This swelling behavior was consistent with the elastic behavior observed. When the entanglements were experimentally accounted for by using the experimentally measured elastic modulus, then the Flory-Rehner model coupled with the phantom network assumption adequately predicts the swelling results over a wide range of swelling extents.

The same method was used to test the swelling of the networks in the solvents 2,3 - dimethylpentane and 2,2,4 - trimethylpentane. These two solvents were unique in that they had interaction parameters, χ's, that were concentration independent of the PDMS networks and had a greater network swelling capability than toluene and benzene. Their interaction parameters at infinite dilution, χ_0, were determined using intrinsic viscosity data of uncrosslinked PDMS chains and the Stockmayer-Fixman relationship assuming the universal viscosity constant was 2.0×10^{23} mol^{-1}. The interaction parameters calculated from the Flory-Rehner model assuming the phantom network were nearly independent of the concentration and gave good agreement with the value of χ_0 determined from the intrinsic viscosity data. Although these solvents swelled the networks to a greater extent than toluene and benzene, excluded volume effects were small enough not to cause deviations from Flory-Rehner.

Networks swollen to equilibrium with polymer chains gave similar correlations between υ_2 and M_c as above. However, the molar volume of the polymer chain solvent, $N_1 v_1$, needed to fit the experimental data was much lower than the theoretical prediction.

Small angle neutron scattering (SANS) of interpenetrating networks (IPNs) were performed to study the conformations of the linear chain within the network and study the effect of crosslinks on the stability of the IPN. A method to synthesize the deuterated monomer, hexamethylcyclotrisiloxane, used in the SANS experiments is given. The SANS results showed that the IPN with the higher crosslink density scattered neutrons more intensely than that of the IPN with a lower crosslink density. When these two different IPNs were compared to the equilibrium swelling curve, it was shown that the former was prepared in a region close to being unstable whereas the latter was clearly in the single phase region. The instability of the former would give the increased scattering observed from neutron scattering.

BIOGRAPHICAL SKETCH

Shawn Malone was born in Tacoma, Washington on September 23, 1965. He attended Maur Hill Prep School in Atchison, Kansas where he graduated as valedictorian in 1983. He received a B.S. in Chemistry from Missouri Western State College, with honors, in 1987. At that time, he accepted a commission as a second lieutenant in the United States Army Chemical Corps and entered active duty. His first assignment was with the 101st Airborne (Air Assault) Divison where he served as a battalion chemical officer and air defense platoon leader. Shawn was selected by the Army to participate in a fully-funded graduate program called the Technological Enrichment Program (TEP) in 1990 at which time he entered the School of Chemical Engineering at Cornell University. Captain Shawn Malone will return to the Army where he will continue his career in the Chemical Corps.

to my wife, Cathy

and sons, Corey and Kyle

ACKNOWLEDGMENTS

I would first like to thank the Department of the Army for allowing me to attend graduate school while on active duty, in the fully-funded program. In addition, I am sincerely thankful for having a thesis advisor as patient, supportive, understanding, enthusiastic, and energetic as Dr. Claude Cohen. Through him I was able to complete my work in a focused and timely manner. I would also like to thank Dr. Ferdinand Rodriguez for serving on my special committee.

Special thanks to Ralph Colby in performing the dynamic mechanical experiments conducted at Kodak Corporate Research Laboratories and to Barry Bauer and Robert Briber in performing the small angle neutron scattering experiments at the National Institute of Standards and Technology.

Of all the people that were supportive, none could ever match that of my wife Cathy. She was the one that was there for me when I was frustrated with my studies or had to work late to complete my work. Her ultimate gift to me while at Cornell was the birth of our son Kyle born July 7, 1992. My son Corey also helped me through the tough times by keeping me preoccupied playing Legos and wrestling in the house.

Finally, I would like to acknowledge the friends that my family and I have met while attending Cornell, who all helped make our two years here enjoyable.

TABLE OF CONTENTS

TABLE OF CONTENTS CONTINUED

LIST OF TABLES

LIST OF FIGURES

LIST OF FIGURES CONTINUED

CHAPTER ONE
ELASTIC AND SWELLING PROPERTIES OF ENDLINKED NETWORKS

1.1 Introduction

When polymer chains are chemically crosslinked or linked at junction points, a three dimensional network of interconnected chains is produced. When a stress is applied to the network its chains rearrange into different configurations than at equilibrium and the network deforms. When the stress is released the non-equilibrium configurations achieved under stress provide the driving force to return the network to its original dimensions. This elasticity is accomplished without any chemical bonds being broken. Over the last 50 years, attempts have been made to model the elastic behavior of polymer networks at a molecular level. However, the increasing number of experiments performed on networks has challenged the validity of these models. One of the most difficult problems in evaluating the models with experiments lies in the knowledge of a polymer network structure and its relation to its mechanical properties. The classical method of crosslinking by irradiation or by chemicals results in polymer chains randomly joined along their contour to produce a network. Unfortunately, these methods produce networks with many defects such as elastically ineffective chains (loops and pendant chains) and entanglements (network chains wrapped around each other such that they cannot deform independently. Recently, attention has been given to endlinked polymer networks which are prepared by linking difunctional polymer

chain ends to multi-functional crosslinkers. These networks tend to have a minimal amount of elastically ineffective chains and have structures that are more easily defined. This has allowed them to be used extensively in evaluating and testing the various molecular models. In the following sections, both classical and recent molecular theories of rubber elasticity are discussed along with the theory of equilibrium network swelling. A description of the synthesis of the polymer precursors and networks will be given with the methods used to characterize these networks. The data obtained will be used to test the molecular theories and will be compared with previous work.

1.2 Molecular Theory of Networks

The classical molecular models proposed relate molecular deformation of the network chains to the macroscopic deformation of the network. The basic premise is that elasticity is entropic in nature. The change in entropy which occurs during a deformation is calculated based on a molecular model and its assumptions. From this entropy change, an elastic modulus can be calculated. A brief review of the original models is given below in addition to more recent models that include entanglement effects.

1.2.1 Affine and Phantom Network Theories

The affine network model, developed by Wall[1] and Flory[2,3] is based on the following assumptions I) the internal energy of the network is independent of chain conformation, II) individual chains between crosslinks obey Gaussian statistics, III) the total number of

conformations of the network is the product of the number of conformations of the individual chains IV) no change in the total volume occurs upon deformation, and V) the crosslinks are firmly embedded in the network and will undergo displacements proportionately to the macroscopic strain (affine deformation). From the above assumptions, the change in entropy for a network deformed uni-axially can be derived[3] as

$$\Delta S = -\frac{Nk}{2}(\alpha^2 + 2\alpha^{-1} - 3) \qquad (1)$$

where k is Boltzmann's constant, N is the number of elastic chains, and α is the elongation (L/L_0) in the deformed direction, where L_0 is the undeformed length of the network. For an ideal rubber, where the internal energy change upon deformation is neglected, the elastic retractive force is[3]

$$f = -\left(\frac{T}{L_0}\right)\left(\frac{\partial S}{\partial \alpha}\right)_{T,V} \qquad (2)$$

From Eq. (1) then,

$$f = \frac{NkT}{L_0}(\alpha - \alpha^{-2}) \qquad (3)$$

This equation can be written in terms of stress, σ, based on the cross-sectional area of an undeformed sample of volume V as

$$\sigma = \frac{NkT}{V}(\alpha - \alpha^{-2}) = \nu kT(\alpha - \alpha^{-2}) \qquad (4)$$

where ν is the number of elastic chains per unit volume. The equilibrium elastic modulus, G_e, that relates stress to deformation is then defined as

$$G_e^{affine} = \nu kT \qquad (5)$$

for the affine network model.

The network model proposed by James and Guth[4,5] has the same assumptions as the affine network except for assumption V. Instead of the crosslinks being fixed, they now could fluctuate about a mean position. James and Guth[6] demonstrated that for these "phantom" networks i) the fluctuations are Gaussian about their mean positions and are independent of the deformation ii) the displacements of the mean positions are affine in the strain, and iii) the fluctuations are smaller as the number of chains linked at a junction (crosslink) increase. The effect of these fluctuations on the entropy change[7] for a uni-axially deformed network is

$$\Delta S = \frac{\xi}{2}(\alpha^2 + 2\alpha^{-1} - 3) \qquad (6)$$

where ξ is the cycle rank of the network, i.e. the number of cuts required to reduce the network to an acyclic tree and is related to the network structure by

$$\xi = (\nu - \mu) \qquad (7)$$

where μ is the number of junctions per unit volume and is related to ν by $\mu = 2\nu / f$, with f being the functionality of the network. From Eq. (2) and (6)

$$f = \frac{(\nu - \mu)kT}{L_o}(\alpha - \alpha^{-2}) \qquad (8)$$

and

$$\sigma = (\nu - \mu)kT(\alpha - \alpha^{-2}) \qquad (9)$$

Then for a phantom network

$$G_e^{phantom} = (\nu - \mu)kT \qquad (10)$$

Comparison of Eqs. (5) and (10) indicate that the phantom and affine molecular models only differ by a factor dependent on functionality. For a tetrafunctional network, this factor is 1/2. Neither of the above models take into account interchain interactions such as chain entanglements.

1.2.2 Constrained Junction and Slip-link Models

In the late seventies, Flory[7] acknowledged that the James and Guth network theory was the best model for larger extensions. This led to the development of the Flory-Erman constrained junction model[8-10] which considered the role of entanglements in the network. In this latter model, the net effect of network entanglements is to reduce the fluctuations of the crosslink junctions; entanglements do not contribute directly to the modulus of a network. At small strains, the entanglements prevent the crosslinks from fluctuating and the network behaves affine-like. At higher strains, the constraints from the entanglements are less pronounced and phantom network behavior is observed. Thus, the modulus predicted by the constrained junction model lies between that of the affine and phantom models.

The theories presented thus far have only considered contributions

to the modulus from the crosslink junctions. The Edward's slip-link model[11-13] considers interactions along the chain contour. These interactions or entanglements are modeled as slip-links joining polymer chains together and may contribute directly to the modulus. The slip-links may either act as chemical crosslinks or can be elastically ineffective. Unlike the constrained junction model, this model predicts moduli which may exceed those predicted by the affine network model due to the additional contribution of entanglements modeled as slip-links.

1.2.3 Flory-Rehner Swelling Model

Because of a network's three-dimensional structure, it will not dissolve in a solvent. However, when placed in a good solvent it will absorb this solvent and swell isotropically until it reaches an equilibrium between the thermodynamic forces trying to dissolve the chains and the retractive elastic force holding the chains together. This swelling has been described by Flory and Rehner[14,3] in a model which is based on the assumption that the free-energy of mixing and the free energy of elasticity are additive,

$$\Delta A = \Delta A_{mix} + \Delta A_{el} \qquad (11)$$

ΔA_{mix} is the free energy due to mixing polymer chains and solvent molecules, and ΔA_{el} is the contribution due to the expansion of the network. The polymer solution theory of Flory[15] and Huggins[16] is used for the ΔA_{mix} term, given by

$$\Delta A_{mix} = kT(N_1 \ln \upsilon_1^* + N_2 \ln \upsilon_2^* + \chi N_1 \upsilon_2^*) \qquad (12)$$

where N_1 and N_2 are the number of solvent and polymer molecules respectively; υ_1^* and υ_2^* are the volume fractions of the components and χ is the polymer-solvent interaction parameter. From Eq. (11) and (12), the difference in chemical potential between the pure solvent, μ_1^o, and the solvent in the swollen network, μ_1, is calculated as

$$\mu_1 - \mu_1^o = kT[\ln(1 - \upsilon_2^*) + \upsilon_2^* + \chi \upsilon_2^{*2}] + \left(\frac{\partial A_{el}}{\partial N_1}\right)_{T,P} \qquad (13)$$

For a network swollen to equilibrium, $\mu_1 = \mu_1^o$, and Eq. (13) gives

$$\ln(1 - \upsilon_2) + \upsilon_2 + \chi \upsilon_2^2 = v_1 \nu \left[\frac{\upsilon_2}{2} - \upsilon_2^{1/3}\right] \qquad (14)$$

for the tetrafunctional affine network model and

$$\ln(1 - \upsilon_2) + \upsilon_2 + \chi \upsilon_2^2 = -v_1 (\nu - \mu) \upsilon_2^{1/3} \qquad (15)$$

for the phantom network model, where υ_2 is the polymer volume fraction at equilibrium swelling, and v_1 is the molar volume of solvent. The difficulty arising from using Eq. (14) or (15) is the determination of the number of elastic chains, ν, or the cycle rank, $\nu - \mu$. For an ideal perfect network prepared by endlinking, each precursor molecule is assumed to become an elastic chain and therefore, ν and μ are well defined and the modulus predicted by the models (Eqs. 5 and 10) can be calculated. However, in real networks, there are always defects present, such as pendant chains (chains attached to one junction only) and trapped entanglements which are not easily quantified. The

former will decrease the modulus, whereas the latter will increase the modulus.

1.3 Experimental Methods

In this section, the methods used to synthesize the polymer precursors and the networks will be described. The mechanical and swelling experiments performed on the networks will also be described. Two different types of precursors are synthesized to give variations in network structure. "Model" networks are formed by endlinking difunctional polydimethylsiloxane (PDMS) chains, denoted as B_2 to tetrafunctional crosslinker molecules (A_4). Variations in structure are obtained by varying the molecular weight of the B_2 precursors and by increasing the number of pendant chains by endlinking monofunctional PDMS (B_1) with B_2 and A_4 to form "imperfect" networks. Both "model" and "imperfect" networks have reasonably well-controlled structures that are helpful in evaluating the theoretical models. A brief review of the synthesis of the precursors and networks is given below; a more detailed description can be found elsewhere[17].

1.3.1 Synthesis of Precursors

The methods of Lee and Johannsen[18-21] were used to synthesize the difunctional precursor (B_2). The monomer, hexamethylcyclotrisiloxane, (D_3), was polymerized in toluene solution using benzyltrimethylammonium bis (o-phenylene dioxy) phenylsiliconate as the catalyst, dimethylsulfoxide (DMSO), as a

promoter, and water as the initiator. D_3 was purified by sublimation[17], the toluene was dried with sodium metal and distilled prior to use and the DMSO was dried with molecular sieves. The catalyst was prepared using the method of Frye[22]; 0.12 moles of catechol, 0.06 moles of phenyltrimethoxysilane, and 10g of methanol were added to a round bottom flask to which benzyltrimethylammonium hydroxide (0.06 moles) in methanol solution were added. The siliconate salt precipitates as white crystals and was purified by recrystallizing twice from hot methanol. The white needle-like crystals were dried in a vacuum oven and stored in a dessicator.

It has been observed that the molecular weight of the polymer synthesized by the above procedure was inversely proportional to the amount of water reacted rather than to the amount of catalyst added[19]. To synthesize networks of high molecular weight care must be taken to ensure the system is dried so that the only water in the system is added intentionally. Therefore, the polymerization was carried out in a round bottom flask that had been repeatedly flame dried to remove as much water from the glass surface as possible. This process involved repeatedly heating the system, purging with nitrogen, and evacuating the gas with a vacuum pump. The flask was equipped with a rubber septum and a magnetic stir bar. After the flask had cooled, purified D_3, dissolved in an equal mass of distilled toluene and a small amount of water were added. To obtain precursors with a number average molecular weight, M_n, greater than 50,000 the ratio of water to monomer, $\mu L\ H_2O/\ g\ D_3$, should be less than 0.1. For low molecular

weight precursors (M_n < 10,000) a ratio of μL H_2O/g D_3 > 2.5 was used. The flask was placed in a water bath at 55 °C to which the catalyst (0.02%) dissolved in the promoter, DMSO (4%) was added via the septum. The mixture turned cloudy after this addition. After approximately two hours, the polymerizations were stopped. To functionalize the polymer chain ends with vinyl groups, an excess of vinyldimethylchlorosilane dissolved in toluene was added after an addition of pyridine. The pyridine acts as an acid scavenger. The polymer was washed several times with water in a separatory funnel to remove any unreacted chlorosilane and then dissolved and reprecipitated with toluene and methanol three times. The final product is dried in a vacuum oven at 60 °C for three days to remove any residual solvents.

The monofunctional precursor, B_1, was synthesized by polymerizing D_3 in cyclohexane, using n-BuLi as an initiator and DMSO as a promoter. The system is prepared as in the B_2 polymerization to ensure all moisture is removed. In a round bottom flask, 20g of purified D_3 was dissolved in 16g of reagent grade cyclohexane, previously dried with calcium hydride, and added to the flask through the rubber septum. The flask was placed in a water bath at 33 °C during the polymerization. A measured quantity of 2.0M n-BuLi in cyclohexane solution was added to get the desired molecular weight. The promoter, DMSO, was added a few minutes afterwards. The polymerization ran for 2 hours after which it was vinyl terminated, washed, and precipitated using the same techniques as for B_2.

The B_2 and the B_1 precursors were characterized by gel permeation chromatography (GPC) at Eastman Kodak Company. Toluene was used as the carrier solvent and polystyrene standards were used to calibrate the instrument. The PDMS "polystyrene equivalent" molecular weights were corrected using a universal calibration technique using the Mark-Houwink parameters obtained by Lapp et al.[23] The results are reported in Table 1.1.

1.3.2 Synthesis of Networks

The networks were formed using a well established hydrosilation reaction[24-26] - the vinyl groups at the ends of the polymer molecules react with the silane groups of the crosslinker molecule, tetrakis(dimethylsiloxy) silane (A_4) in the presence of a platinum catalyst, cis-dichlorobis(diethyl sulfide) platinum II as shown by the following reaction

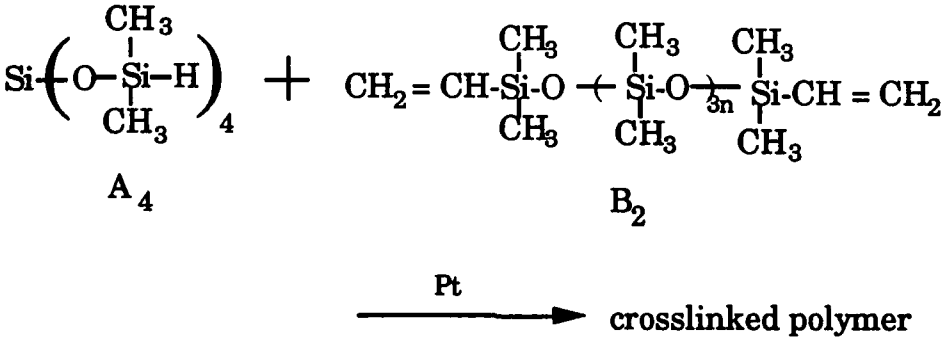

To form model networks, the ratio of silane hydrogens to vinyl groups, r, that gives networks with the lowest degree of equilibrium swelling (high υ_2), was determined. This technique is described in detail elsewhere[17]. In brief, a series of weight ratios of A_4 to B_2 are prepared and mixed overnight in polypropylene vials. The catalyst, dissolved in

Table 1.1

Molecular Weight of PDMS Precursors

sample	M_n	M_w / M_n	f [1]
25A	2,460	1.15	2
43A	6,160	1.17	2
32A-1	8,350	1.25	2
37A	58,000	1.25	2
40B	71,200	1.70	1

[1] functionality of polymer chains

toluene, was added to the vials to achieve a concentration of 20 parts platinum per 10^6 parts PDMS. The mixtures are mechanically stirred and then degassed under a vacuum to remove air bubbles. The samples were cured in a vacuum oven for three days at 35 °C. The networks were removed and swollen in toluene to find the optimum ratio of A_4 to B_2.

The imperfect networks were prepared by mixing known amounts of B_2 and B_1 such that the mole fraction of B_1, x, ranged from 0 to 0.65. The r value used for the preparation of these imperfect networks was kept close to the optimum r used for the preparation of a model network using the same B_2.

1.3.3 Mechanical Experiments

A Rheometrics System Four mechanical spectrometer was used to measure the modulus of the networks. The experiments were performed by Dr. Ralph Colby and Jeffrey Gillmor at the Corporate Research Laboratories of Eastman Kodak Company. The samples were prepared as described above, but after mixing in the catalyst, samples were poured directly onto the lower plate of the rheometer. The samples were then cured between the parallel plates in an inert (N_2) atmosphere at 30 °C.

For dynamic mechanical oscillatory experiments, the stress in the sample can be derived[27] as

$$\sigma(t) = \gamma^0[G'(\omega)\sin(\omega t) + G''(\omega)\cos(\omega t)] \qquad (16)$$

where γ^0 is the maximum amplitude of the strain, ω is the frequency of

oscillation, $G'(\omega)$ is the shear storage modulus and $G''(\omega)$ is the shear loss modulus. For polymer networks, the equilibrium shear modulus, G_e is equal to $\lim \omega \to 0$ of $G'(\omega)$. Experimentally, $G'(\omega)$ for networks is constant over a wide range of ω and this value is taken as G_e.

1.3.4 Swelling Experiments

After the networks were removed from the rheometer, standard techniques[28] were used to extract the soluble material, and to determine the equilibrium polymer volume fraction of the swollen networks. The extraction of sol from the network was carried out over three days using toluene as the solvent. The network was then slowly deswollen using increasing mixtures (15-45%) of methanol in toluene. The network was air dried and placed in a vacuum oven at 60 °C. The weight fraction of soluble material was determined using

$$w_{sol} = \frac{m - m^*}{m} \qquad (17)$$

where m is the mass of the network before extraction and m* is the mass of the network after the soluble material had been extracted. The polymer volume fractions at equilibrium, υ_2, of the networks swollen in toluene and benzene after the extractions were determined gravimetrically at 25 °C. The equilibrium polymer volume fraction, υ_2, can be calculated from the following expression assuming that the polymer and solvent volumes are additive:

$$\upsilon_2 = \left[1 + \left(\frac{m_s^* - m^*}{m^*} \right) \left(\frac{\rho_{2,25^oC}}{\rho_{1,25^oC}} \right) \right]^{-1} \qquad (18)$$

where m_s^* is the mass of the swollen network after sol extraction and $\rho_{2,25^oC}$ and $\rho_{1,25^oC}$ are the densities of polymer and solvent respectively at 25 °C.

1.4 Results and Discussion

1.4.1 Characteristics of the Network Used

Both model and imperfect networks were prepared using the methods outlined in section 1.3.2. The model networks were prepared using B_2 precursors with molecular weights less than M_n=10,000 and greater than M_n=54,000. These molecular weights were chosen to supplement the data of Patel[17] whose work included molecular weights ranging from 10,300 to 53,500. The molecular weights of the precursors used to synthesize the networks used here were chosen to observe the effect of entanglements on the modulus of networks with a higher density of elastic chains than those of Patel and to see if the value of the modulus of networks with a lower density of elastic chains remained constant.

The networks used in this work exhibited minimum extent of swelling in a narrow range of A_4 / B_2 ratios in the preparation recipe. Plots of υ_2 versus r, where r = 4 x mol A_4/(2 x mol B_2 + mol B_1), are shown in Fig. 1.1. They indicate that a maximum in υ_2 is obtained at r greater than 1. For the molecular weight precursors with M_n less

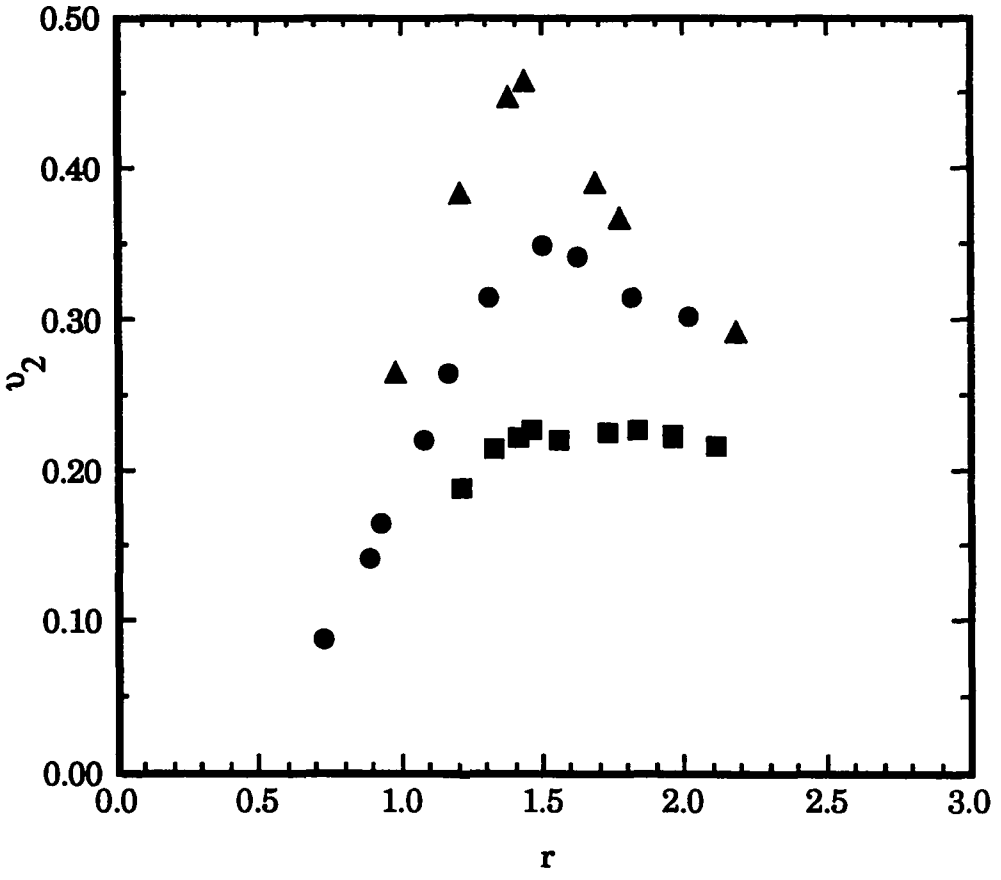

Figure 1.1. Plot of υ_2 versus r used to determine the optimum r needed to give minimum swelling. The symbols ▲, ●, and ■ correspond to the networks made with B_2 precursors with number average molecular weights of 2460, 6160, and 58000 respectively.

than 7000, the optimum r's, r_{opt}, were 1.44 and 1.50 which were slightly lower than that of the network prepared with B_2 with a molecular weight of 58,000 (sample A-4) which had an r_{opt} at 1.61 and gave a broader maximum. The stoichiometric ratio of one silane hydrogen for each vinyl group gives r equal to unity; however unequal reactivity of the reactive sites of an A_4 molecule due to steric hindrance probably leads to the larger values of r needed to form tighter networks. These results are consistent with the work of Patel[17] and supports the suggestion that smaller polymer molecules will diffuse more easily to a reactive site on a given partially reacted A_4 molecule, than a larger polymer molecule and therefore decreasing the amount of A_4 needed to form the optimum network from low molecular weight precursors. The molecular weight of the precursors, equilibrium polymer volume fraction in toluene, υ_2, and weight fraction of soluble material, w_{sol}, are reported in Table 1.2 for the model networks. The imperfect network series were prepared using mixtures of B_2 with M_n = 58,000 and B_1 with M_n = 71,200. The molar fraction of monofunctional precursors, x, ranged from zero to 65%. The characteristics of the imperfect networks are given in Table 1.3.

1.4.2 Elastic Behavior of Model and Imperfect Networks

Plots of G' and G" versus frequency, ω, for the model networks are consistent to those observed in earlier work[17] where G' is observed to be constant over frequencies ranging from 10^{-2} to 100 rad/sec and having values an order of magnitude greater than those of G" as shown for sample A-4 in Fig. 1.2. The equilibrium modulus, G_e, is taken to be

Table 1.2

Experimental Characteristics of Model Networks

network designation	M_{n,B_2}	r	$w_{sol} \times 10^2$	υ_2	G_e/RT (mol/m^3)	$G_e/RT(1-w_{sol})^{1/3}$ (mol/m^3)
A-1	2,460	1.44	0.374	0.442	303	303
A-2	6,160	1.51	0.281	0.354	184	184
A-3a	8,350	1.72	0.450	0.317	149	149
A-3b	8,350	1.61	0.436	0.326	154	154
A-4	58,000	1.61	2.63	0.217	74.2	74.9

Table 1.3

Experimental Characteristics of Imperfect Networks

network designation	x	r	$w_{sol} \times 10^2$	υ_2	G_e/RT (mol/m^3)	$G_e/RT(1-w_{sol})^{1/3}$ (mol/m^3)
B-1	0	1.61	2.63	0.217	74.2	74.9
B-2	0.170	1.47	6.98	0.183	35.6	36.5
B-3	0.336	1.49	14.5	0.143	21.8	23.0
B-4	0.482	1.44	27.8	0.094	11.8	13.2
B-5	0.622	1.42	39.6	0.066	4.45	5.26

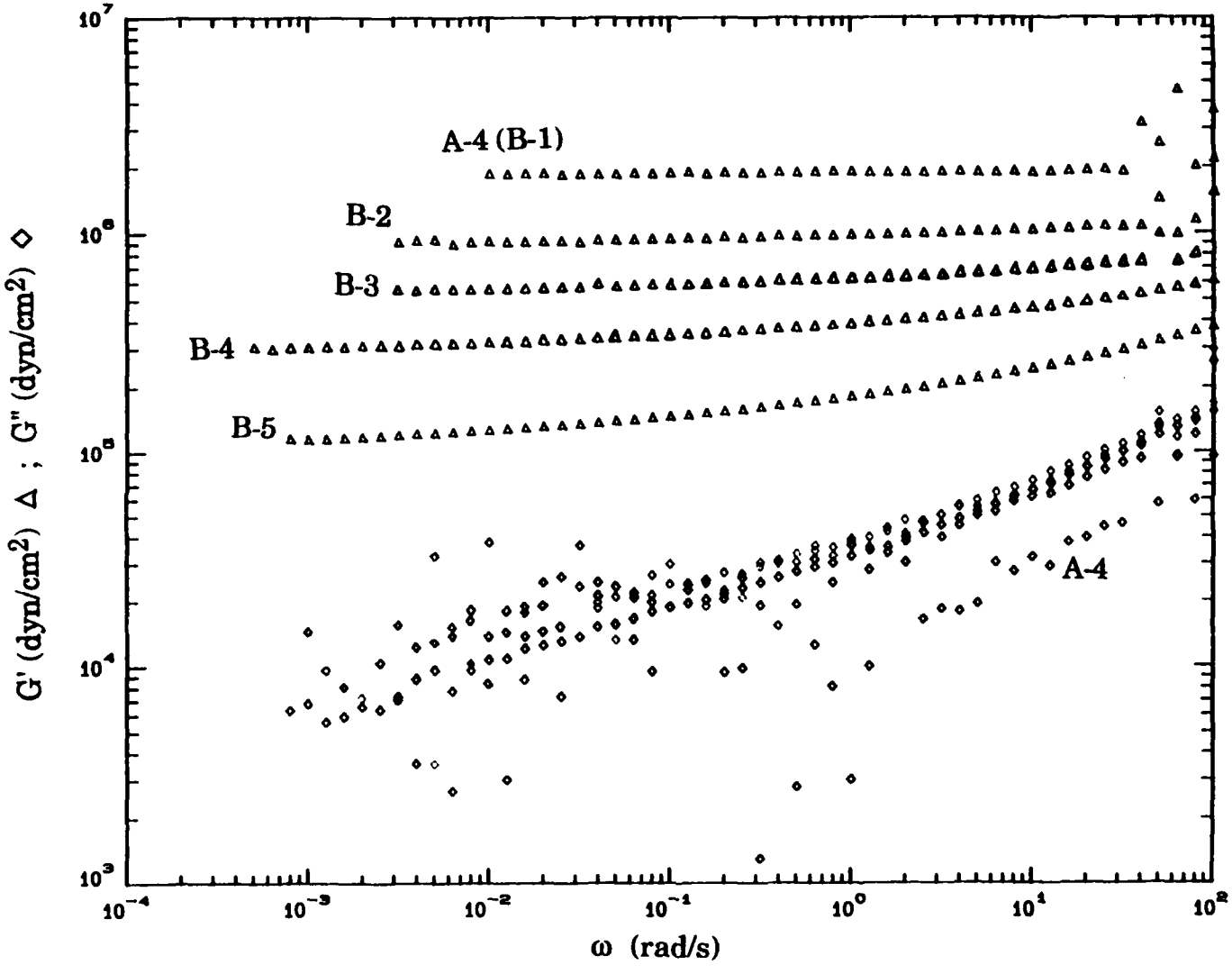

Figure 1.2. Plots of G'(ω) and G"(ω) versus ω for the model network A-4 and the imperfect networks (B-2 to B-5) made from the same B_2 precursor as sample A-4.

equal to G' for the model networks. The values of G' are recorded in units of dyne/cm^2 and are reported in Table 1.2 as G_e/RT in units of mol/m^3.

For the imperfect networks plotted in Fig. 1.2, a noticeably different behavior is observed. When a small amount of B_1 precursors (x= 0.170) are added to the model network, the value of G' decreases and G" increases, indicating an increase in the viscous response of the sample. As x is increased the value of G' continues to decrease, but G" remains relatively the same and the ratio G'/G" decreases. Imperfect network samples B-4 and B-5, which have high values of x (high mole fractions of B_1 precursors), show clearly a relaxation in G' at high frequencies as shown in Fig. 1.2. This relaxation was not observed in Patel's results[17] because of the lower extent of pendant chains in this work, but was observed by in trifunctional PDMS networks with large amounts of pendant chains[38]. The mechanical measurements performed here were done on the networks prior to the removal of the sol fraction which acts as a diluent. Therefore, both the sol fraction and the increasing amount of pendant branched structures of the network are relaxing during the measurement of the elastic modulus. In the case of these imperfect networks, G_e is taken as the asymptotic value of G' at low frequency.

To correct for the effect of sol on the values of the elastic modulus, we can use an expression derived by Flory[3] for networks swollen in a solvent. For an affine network this expression is

$$\frac{G_e}{RT} = \nu \upsilon_2^{1/3} \qquad (19)$$

where G_e is based upon the swollen dimensions. The volume fraction of polymer, υ_2, of a network sample prior to sol extraction is given by

$$\upsilon_2 = 1 - \upsilon_{sol} = 1 - w_{sol} \qquad (20)$$

since the density of the sol fraction is equal to the density of the network chains. The value of the modulus of the dry network after extraction is then obtained from Eqs (19) and (20) as:

$$G_{e,\,corrected} = \frac{G_e}{(1-w_{sol})^{1/3}} = RT\nu \qquad (21)$$

This correction also applies to the phantom network model if $(\nu - \mu)$ is substituted for ν. As seen in Tables 1.2 and 1.3 this correction is extremely small for the model networks (< 1%) and is still reasonably small for the imperfect networks (< 20%). For the figures presented here, the uncorrected values of G_e/RT will be used.

To compare the experimental values of G_e with the theoretical models, the number of elastic chains, ν, per unit volume of network must be determined. Many workers have assumed that ν can be expressed as $\rho_2/M_{n,B_2}$ for endlinked model networks where ρ_2 is the density of the polymer and M_{n,B_2} is the molecular weight of the B_2 precursors. However, this approximation has been shown to be poor, even for networks with very low sol fractions[17]. The Macosko-Miller

model[29-31] of nonlinear polymerization is used to evaluate ν for both the model and imperfect networks. This model is based on elementary probability laws and can be used to derive expressions for the molecular weight of the elastic chains, $M_{n,el}$, the density of elastic chains, ν, and the density of crosslinks, μ,of the networks. These expressions which result from the application of this model to the case of the copolymerization of A_4 with B_2 and B_1 have been derived in detail elsewhere[17] and are listed in Appendix A. The characteristics of the network based on the Macosko-Miller model can be determined from the sol fractions[33] and the relative amounts of the initial reactants (A_4, B_2, and B_1)[17]. The Macosko-Miller structure parameters found for the model and imperfect networks prepared here are listed in Tables 1.4 and 1.5 respectively. The ν values calculated from the Macosko-Miller model for the model networks are much lower (40 - 60%) than those calculated from the density. There are a couple of reasons for this difference. First, the networks have a functionality less than four as shown by the ratio μ/ν in column four of Table 1.4 ($f=2\nu/\mu$). This is consistent with the values of optimum r obtained in section 1.4.1. The ratio, μ/ν, should be 1/2 for ideally perfect tetrafunctional networks. Also in any given preparation method a certain amount of pendant chains will be present, even in model networks. For the imperfect networks listed in Table 1.5 we see that the average functionality decreases (μ/ν increases) as expected, as more pendant material (B_1) is added.

In Figure 1.3, the experimental values of G_e/RT for the model networks reported here in Table 1.2 and those of Patel's earlier work[17]

Table 1.4

Macosko-Miller Parameters for Model Networks

sample; M_{n,B_2}	$M_{n,el}$ x 10^{-3} (g/mol)	ν (mol/m3)	$\nu - \mu$ (mol/m3)	μ / ν
A-1; 2460	3.48	242	96.2	0.602
A-2; 6160	8.64	100	39.6	0.604
A-3a; 8350	13.1	64.5	24.7	0.617
A-3b; 8350	12.5	67.7	26.2	0.613
A-4; 58000	102	6.87	2.58	0.624

Table 1.5

Macosko-Miller Parameters for Imperfect Networks

M_{n,B_2} = 58000; M_{n,B_1} = 71200

sample; x	$M_{n,el}$ x 10^{-3} (g/mol)	ν (mol/m3)	$\nu - \mu$ (mol/m3)	μ / ν
B-1; 0	102	6.87	2.58	0.624
B-2; 0.170	109	4.94	1.84	0.629
B-3; 0.336	137	2.75	0.995	0.638
B-4; 0.482	190	1.23	0.436	0.647
B-5; 0.622	261	0.553	0.192	0.653

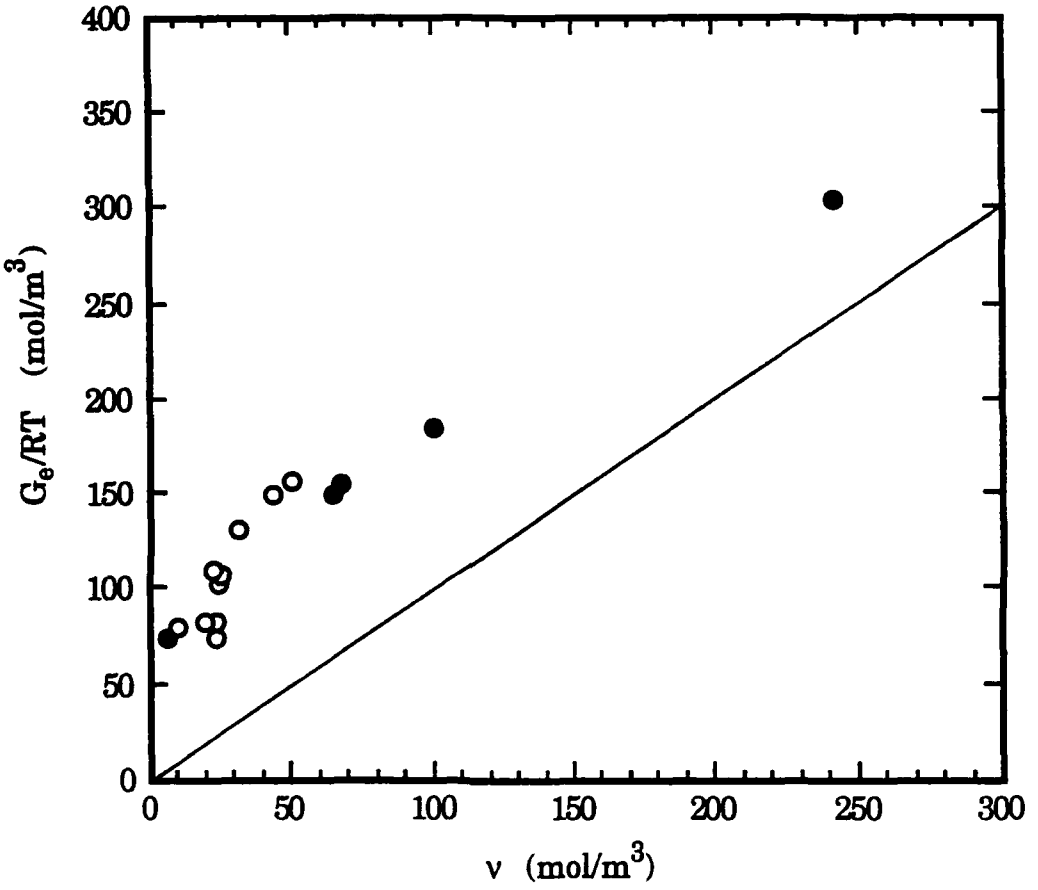

Figure 1.3. Equilibrium shear moduli of model networks plotted as G_e/RT versus ν calculated from the Macosko-Miller model. The straight line represents the behavior predicted by the affine network model. The symbols ● and O represent model networks prepared in the present work (Table 1.2) and from reference 17 respectively.

are plotted versus the values of ν calculated from the Macosko-Miller model. The sol fraction correction of Eq. (21) would only raise the data further above the affine prediction (solid line), but the change would be too small to notice. The model network (sample A-4) prepared from the polymer precursor with M_n=58,000 and ν = 6.3 exhibited essentially the same value of the modulus as that of model networks that had 10.3 < ν < 24 mol/m^3. This value is very close to the plateau modulus of high molecular weight, uncrosslinked PDMS, which has been reported by Plazek et al.[32] and Valles and Macosko[33] to be 2.0 and 2.11 x 10^6 dyn/cm^2, corresponding to values of G_e/RT of 79 and 84 mol/m^3 respectively. Sample A-4 had a relatively high sol fraction (> 2%) as compared to the other model networks which had sol fractions less than 1%. This difference may explain the slightly lower than expected modulus of sample A-4. This result differs significantly from the observation of Opperman and Rennar[34] who saw a sharp decrease in G_e at low ν for endlinked PDMS networks. From the results reported here and from further evidence to come below from our imperfect network series, this previously observed sharp decrease may be caused by network imperfections. These results might also be explained if the networks exhibiting these very low values of G_e have been prepared with a stoichiometric value of r (r $\approx$ 1) rather than the optimum r used here. The moduli of the low molecular weight networks show a linear dependence on ν and parallel the predictions from the affine network model. The results reported here indicate that the affine model fails because chain entanglements and network interpenetration play a significant role in the contribution to the modulus especially for low ν

networks (high molecular weight precursor chains).

In Figure 1.4, the experimental results of the modulus of the imperfect networks prepared here (M_{n,B_2} = 58K, M_{n,B_1} = 71K) are plotted versus the calculated Macosko-Miller ν values from Table 1.3 along with those of Patel's results on imperfect networks formed from mixtures of M_{n,B_2} = 20K and M_{n,B_1} = 20K[17]. The imperfect networks exhibit values of G_e/RT which quickly drop from the plateau value in almost a linear fashion as ν decreases and more B_1 is added. However, the values of G_e/RT of the present imperfect networks decrease faster with ν than those of Patel. This behavior can be explained by comparing the model networks (x=0) from which the imperfect networks originated. Patel's model network B-5 (M_{n,B_2} = 20K) has approximately the same modulus as the present model network A-4 (M_{n,B_2} = 58K), however, since shorter elastic chains trap fewer entanglements than longer elastic chains, the addition of B_1 to sample A-4 releases more trapped entanglements than an equivalent amount of B_1 added to sample B-5. This leads to a faster drop of the modulus and to the experimentally observed results in Fig. 1.4.

1.4.3 Swelling Behavior of Model and Imperfect Networks

Using Eqs. (17) and (18), values of w_{sol} and υ_2 were experimentally determined for each network and are reported in Tables 1.2 and 1.3. In the previous section, it was shown that the affine model underpredicts the modulus of the PDMS networks if the role of trapped entanglements is not taken into account. If the Flory-Rehner model is based on either the affine or phantom network models as in Eqs. (14)

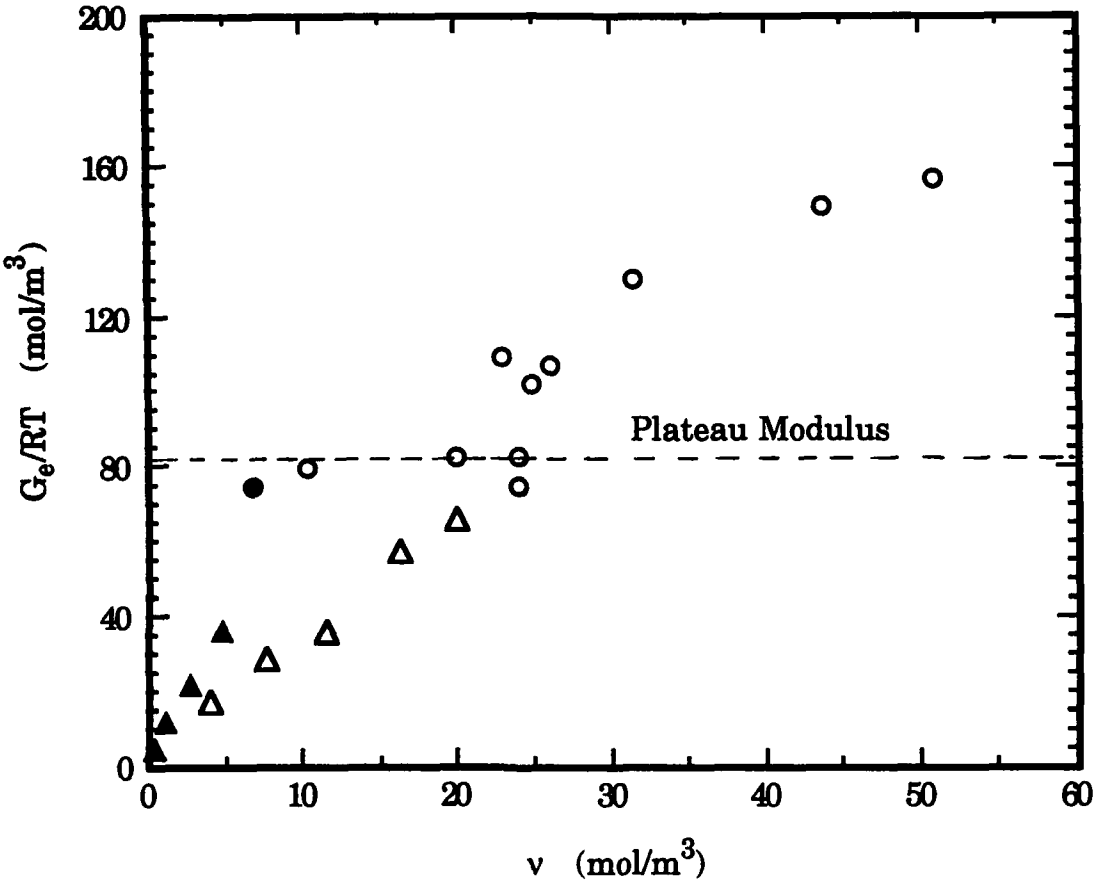

Figure 1.4. Equilibrium shear moduli of all the networks with low ν calculated from the Macosko-Miller model. The circles represent the model networks from Fig. 1.3. The symbols ▲ and Δ represent the imperfect networks from Table 1.3 and from reference 17 respectively. The dashed line is the average value of previously reported plateau moduli from references 32 and 33.

or (15), then it too should fail since neither of the elasticity models account for these interchain interactions or entanglements. This is shown for the swelling results in toluene of the model networks of Table 1.2 and of reference 17 in Fig. 1.5 for the affine and phantom network models respectively. Figure 1.5a is plotted assuming a tetrafunctional network. However, the factor of 1/2 in the denominator of the ordinate for the affine network model should be replaced with μ/ν for networks with a functionality different from 4. Because the use of the calculated values of μ/ν reported in Tables 1.4 and 1.5 instead of 1/2 only results in a minor change (about 5%) in the slopes of the various experimental data and will make the ordinate dependent on the branching model, the factor of 1/2 was used in Fig. 1.5a. The value of $\chi = 0.445 + 0.297\upsilon_2$, obtained from the literature[35] on linear PDMS chains in toluene, was used in the ordinate as well as a value of v_1=106.9 cm^3/mol. The results show that the swelling of the model networks prepared from both low and high molecular weight precursors exhibit a linear dependence on ν. A least-squares regression gives slopes of 1.78 and 3.08 in Figs. 1.5a and 1.5b respectively, and the intercepts of these lines are non-zero, clearly violating the prediction of the models where the slopes should be unity and the intercepts should be zero.

The swelling results from the imperfect networks obtained here (Table 1.3) and those from Patel[17] are plotted in Figs. 1.6a and 1.6b in terms of the Flory-Rehner model. The results from the imperfect networks in this work fall to zero more quickly and have a greater ν dependence than Patel's results. The ν dependence is also much stronger than that observed for the model networks, as indicated by the

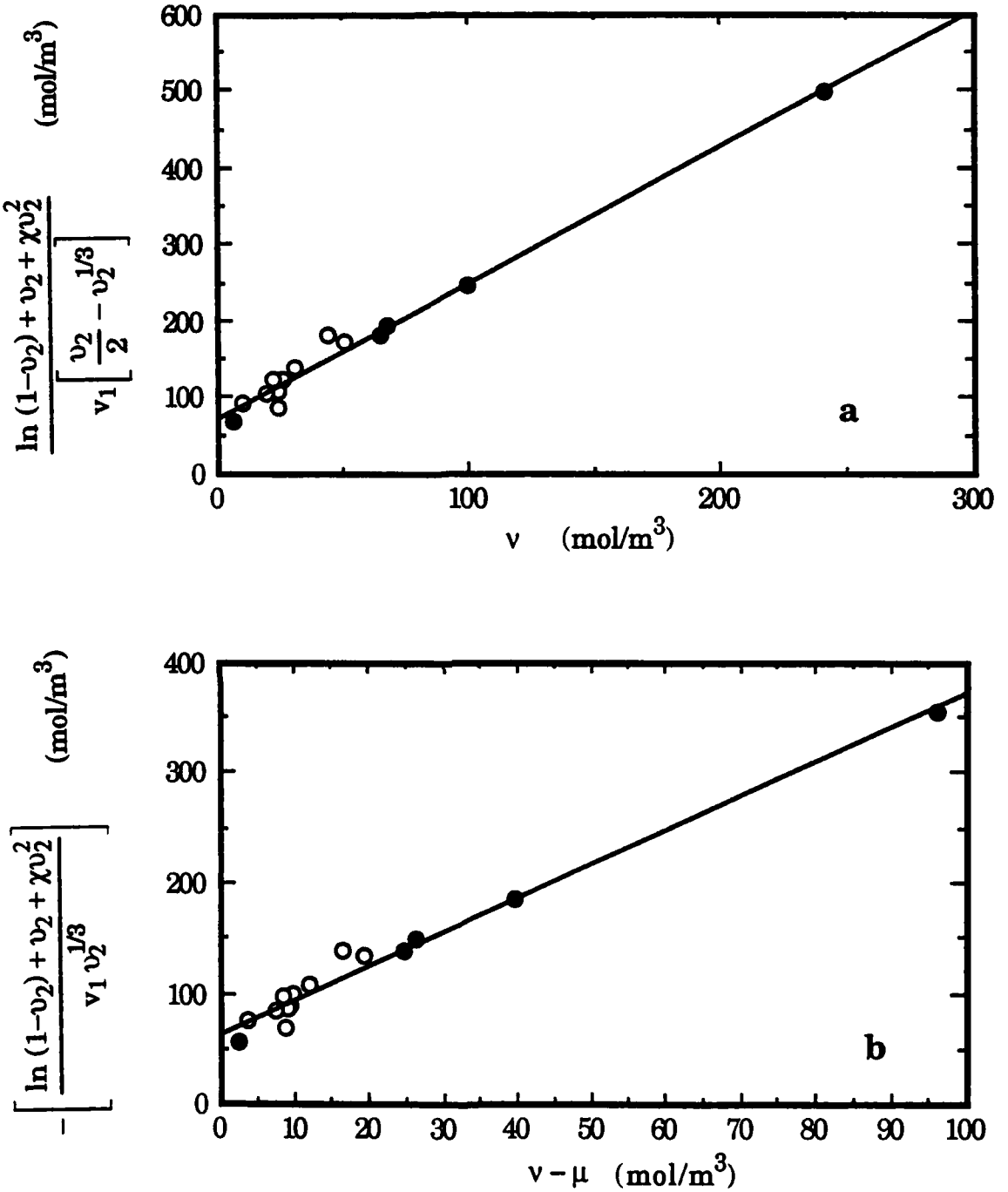

Figure 1.5. a) Test of the Flory-Rehner swelling model for the model networks swollen in toluene assuming the affine network where ν is calculated from the Macosko-Miller model. b) Same as in a) but for the phantom network where ν −μ is calculated from the Macosko-Miller model. The symbols are the same as in Fig. 1.3. Lines are least-squares regression fits to the data.

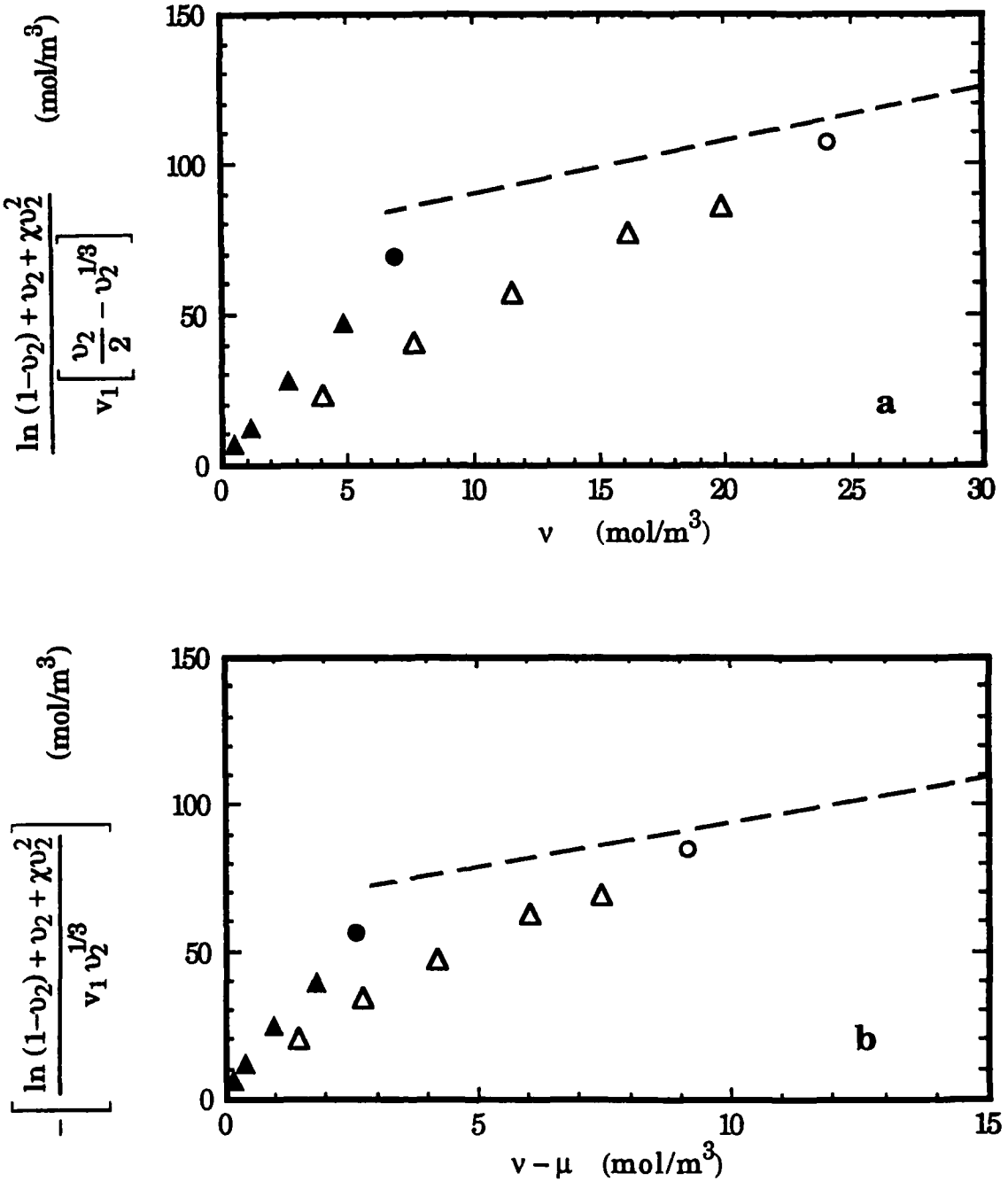

Figure 1.6. a) Test of the Flory-Rehner swelling model for the imperfect networks swollen in toluene assuming the affine network where ν is calculated from the Macosko-Miller model. b) Same as in a) but for the phantom network where $\nu - \mu$ is calculated from the Macosko-Miller model. The symbols are the same as in Fig. 1.4. The dashed lines are best fit lines of the data for model networks in Fig. 1.5.

dashed lines. This swelling behavior is consistent with the elastic behavior observed in section 1.4.2 where the model networks were more effective at trapping entanglements as compared to the imperfect networks and where the high molecular weight precursor (M_{n,B_2} = 58K) used here is trapping more entanglements than its counterpart (M_{n,B_2} = 20K) used in the previous study.

The number of entanglements obviously plays an important role in the relation between mechanical properties and equilibrium swelling and therefore in the validity of the Flory-Rehner model. A method used to include the effect of trapped entanglements on swelling is to replace νRT and $(\nu - \mu)RT$ in Eqs. (14) and (15) with the experimentally measured modulus to obtain[17]

$$\frac{\ln(1-\upsilon_2)+\upsilon_2+\chi\upsilon_2^2}{v_1\left[\frac{\upsilon_2}{2}-\upsilon_2^{1/3}\right]}=\frac{G_e}{RT} \qquad (22)$$

and

$$-\left[\frac{\ln(1-\upsilon_2)+\upsilon_2+\chi\upsilon_2^2}{v_1\,\upsilon_2^{1/3}}\right]=\frac{G_e}{RT} \qquad (23)$$

where G_e is the equilibrium modulus of the unswollen network. Equations (22) and (23) are direct predictions of the original theory of Flory-Rehner where the swelling is a balance between osmotic and elastic forces. Both equations are tested in Figs. 1.7 and 1.8 for both the model and imperfect networks swollen in toluene and benzene. The

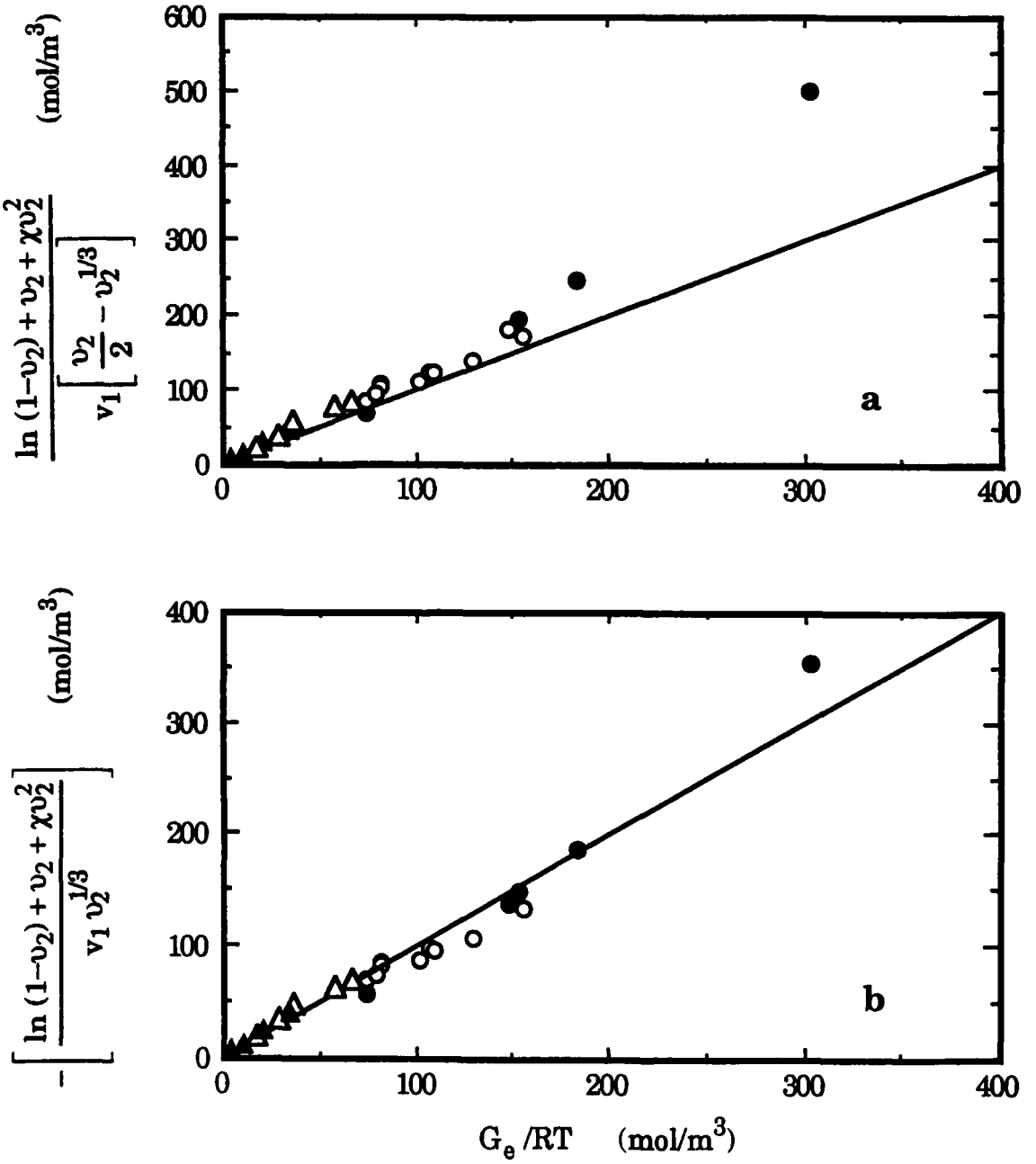

Figure 1.7. Comparison of the swelling results from all the networks in toluene with the Flory-Rehner prediction assuming a) the affine model, and b) the phantom model. G_e in the abscissa is the experimentally determined value of the modulus. The symbols are the same as in Fig. 1.4.

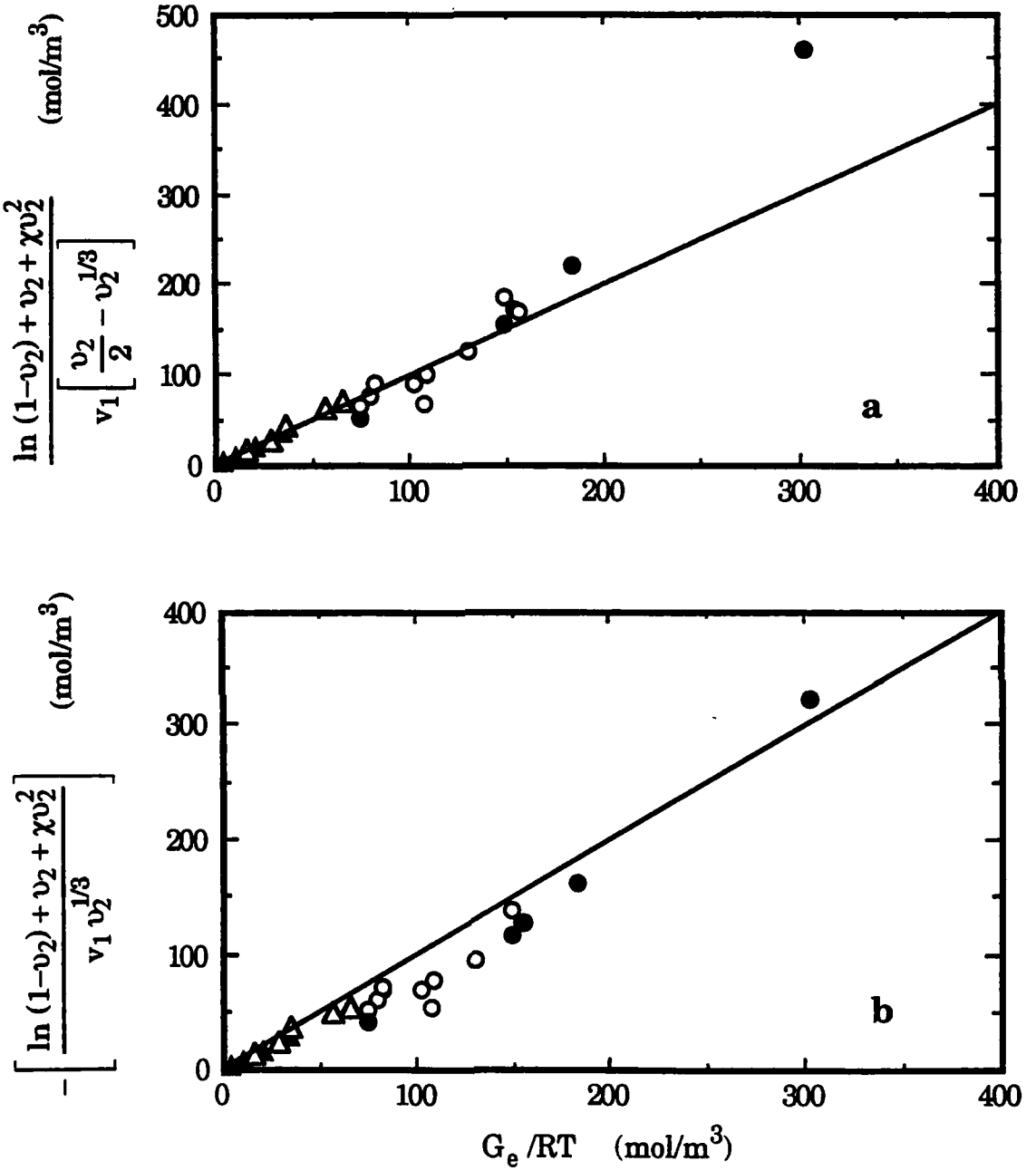

Figure 1.8. Comparison of the swelling results from all the networks in benzene with the Flory-Rehner prediction assuming a) the affine model, and b) the phantom model. G_e in the abscissa is the experimentally determined value of the modulus. The symbols are the same as in Fig. 1.4.

data of reference 17 is also included. The interaction parameter for PDMS-benzene used in these calculations is $\chi = 0.484 + 0.33\upsilon_2$ reported by Flory and Shih[36] and v_1 for benzene is taken as 89.41 cm^3/mol. For both solvents, the Flory-Rehner model based on the phantom network, Eq. (23), gives a better correlation between the swelling and modulus data over the range of equilibrium swelling extents studied here. Equation (22), which is based on the affine model, gives reasonable agreement, except for a larger deviation from the prediction at high G_e and high υ_2 (low swelling). This is due to the fact that Eqs. (22) and (23) only differ on their left-hand sides. The difference is generally negligible since the additional $\upsilon_2/2$ term in Eq. (22) is small compared to the $\upsilon_2^{1/3}$ term for small υ_2's. For higher values of υ_2, the difference increases, and gives the deviation observed. Patel[17] did not see this significant departure from the affine prediction since his highest G_e/RT and υ_2 were 150 mol/m^3 and 0.32, respectively, compared to 300 mol/m^3 and 0.44 in this work. The use of $G_e/RT(1-w_{sol})^{1/3}$ instead of G_e/RT introduces a negligible shift of the imperfect network data to the right.

Literature values of χ determined from uncrosslinked PDMS solutions were used above in Eqs. (22) and (23) to compare the models to the experimental results. These equations can also be used, however, to solve for χ and its dependence on υ_2. Here, only the phantom model (Eq. 23) is used as it gave better agreement with the swelling data in Figs. 1.7b and 1.8b and is also supported by neutron scattering studies of the fluctuations of deuterated crosslinkers in similar endlinked PDMS networks[39]. Figures. 1.9 and 1.10 show the resulting values of

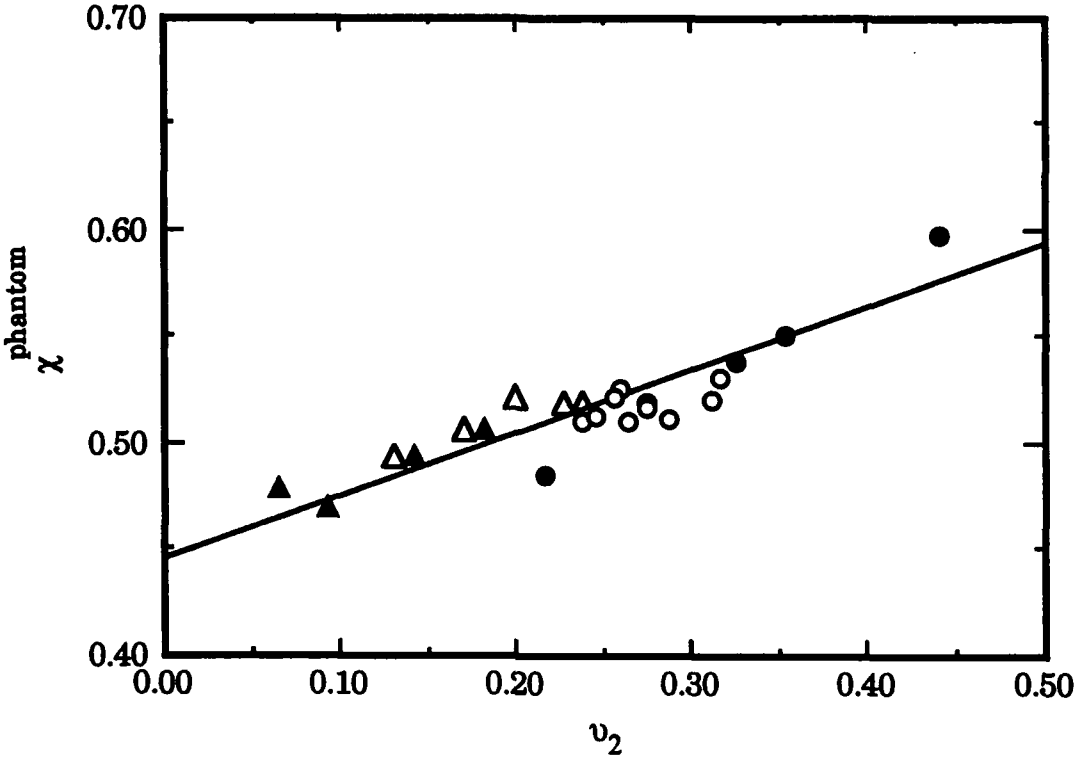

Figure 1.9. χ as a function of υ_2 for the networks swollen in toluene. The values of χ are calculated from the swelling results using the Flory-Rehner model with the phantom network assumption. The symbols are the same as in Figure 1.4. The line represents the interaction parameter obtained for solutions of uncrosslinked PDMS chains in toluene from reference 35.

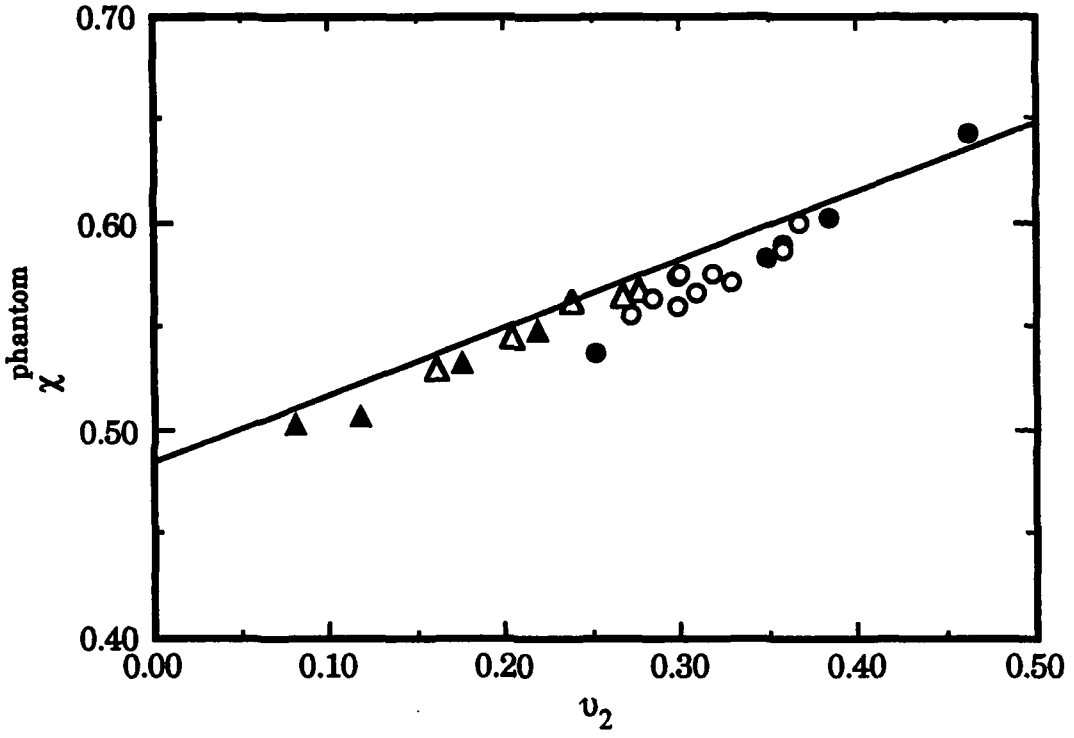

Figure 1.10. χ as a function of υ_2 for the networks swollen in benzene. The values of χ are calculated from the swelling results using the Flory-Rehner model with the phantom network assumption. The symbols are the same as in Figure 1.4. The line represents the interaction parameter obtained for solutions of uncrosslinked PDMS chains in benzene from reference 36.

χ for toluene and benzene respectively. Both figures show clearly that χ is a linear function of concentration for PDMS networks swollen in toluene and benzene in the concentration range studied. A linear regression applied to the data for toluene in Fig. 1.9, gives $\chi = 0.452 + 0.265\upsilon_2$, which is very close to the literature value of χ for PDMS chains in toluene reported earlier and plotted in Fig 1.9 as a solid line. For benzene a best-fit line through the data yields $\chi = 0.470 + 0.337\upsilon_2$.and would lie only very slightly below the previously reported values of χ for uncrosslinked PDMS solutions in benzene.

The effect of entanglements can be incorporated in the evaluation of the molecular weight between "effective" crosslinks, $M_{n,el}$, by equating it to M_c, obtained from the equilibrium elasticity measurements of the unswollen networks. For simplicity, the affine model is used and is written:

$$M_{n,el} = M_c = \frac{\rho_2 RT}{G_e} \qquad (24)$$

This method allows the data from the imperfect networks to be included in calculating M_c. Eq. (24) essentially means that the number density of the effective elastic strands is calculated according to the affine model from the experimental value of the modulus. If the phantom network is assumed, then the right-hand side of Eq. (24) is multiplied by a factor of $(1 - \mu/\nu)$. This factor is approximately constant for the networks and will not appreciably affect the correlation between $\log \upsilon_2$ and $\log M_c$ as shown in Fig. 1.11. A straight line of slope = -0.4 fits the data in Fig. 1.11 reasonably well. This slope is much different

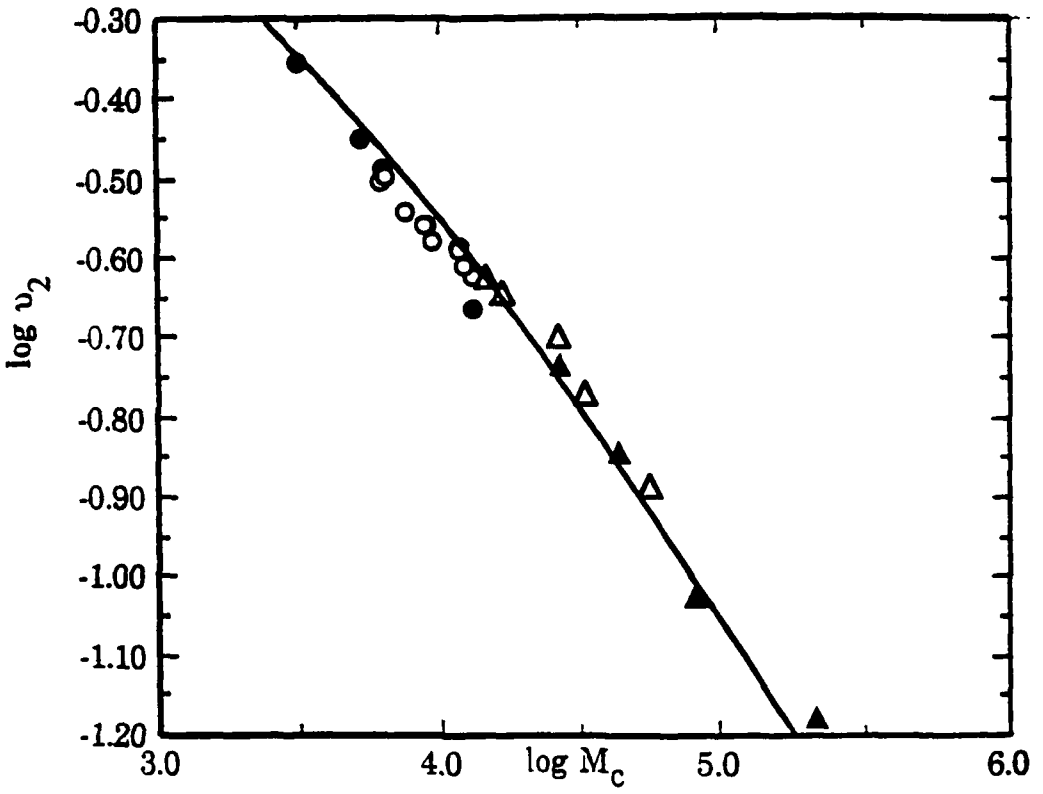

Fig. 1.11. Scaling relationship between υ_2 and M_c for the networks swollen in toluene. The symbols are the same as in Figure 1.4. The curve represents the Flory-Rehner prediction with the phantom network assumption (Eq. 25) and using the χ parameter from reference 35.

from the prediction of the c* theorem[37] where scaling laws predict $\upsilon_2 \sim M_c^{-0.8}$. This is also quite different from the results of Flory-Rehner where $\upsilon_2 \sim M_c^{-0.6}$ in the limit of $\upsilon_2 << 1$. The latter result is obtained by expanding the logarithmic term of the Flory-Huggins expression and keeping only the quadratic terms. However, if the higher order terms in the expansion are kept, the Flory-Rehner expression gives very good agreement with experimental results as was shown above. In Fig. 1.11, the curve is a representation of the Flory-Rehner equation with $\chi = \chi_0 + \chi_1 \upsilon_2$ and the logarithmic term is expanded up to υ_2^4 terms, namely,

$$\frac{\left(\frac{1}{2} - \chi_0\right)\upsilon_2^2 + \left(\frac{1}{3} - \chi_1\right)\upsilon_2^3 + \frac{1}{4}\upsilon_2^4}{\upsilon_2^{1/3}} = \frac{v_1 \rho_2}{M_c} \qquad (25)$$

where the values of χ_0 and χ_1 are taken from reference 35. The good agreement with the Flory-Rehner model implies negligible excluded volume effects in the concentration range investigated; i.e. the chains remain Gaussian and not highly swollen.

1.5 Conclusion

Two types of networks were synthesized. The model networks were prepared using pure B_2 precursors with number average molecular weights, M_n, less than 10,000 and greater than 54,000. The second type of network, referred to as "imperfect", were prepared from mixtures of B_2 and B_1 using M_n = 58,000 for the B_2 precursor and M_n = 71,200 for B_1.

The moduli of the networks were measured using a dynamic mechanical spectrometer. For the model networks, the value of $G'(\omega)$ were constant over a wide range of frequencies and were equated to the equilibrium modulus, G_e. The imperfect networks exhibited the same behavior until the mole fraction of B_1 exceeded 0.35. Here, a relaxation in $G'(\omega)$ was observed at high frequencies. This relaxation comes from a combination of increased amounts of highly branched pendant chains and a contribution from the sol fraction. In this case, G_e was taken as the asymptotic value of $G'(\omega)$ at low frequency.

The experimental values of G_e were compared with the number of elastic chains per unit volume, ν, calculated from the Macosko Miller model of nonlinear polymerization and were found to always lie above the prediction of the affine model. The moduli of model networks made from high molecular weight precursors, remained essentially constant around a value close to the plateau modulus of high molecular weight uncrosslinked PDMS. This indicates that for these networks the major contribution to the modulus is from trapped entanglements. Low molecular weight networks with M_n less than 10,000, had moduli that exhibited a linear dependence on ν that paralleled the affine model prediction. When the values of G_e were plotted against ν for the imperfect networks, a noticeably different behavior was observed. The modulus of the imperfect networks decreased in a linear fashion from the plateau value as more B_1 (pendant material) was added. This effect is attributed to the release of trapped entanglements in the network structure. It was also observed that the addition of B_1 to networks of higher molecular weight

precursors decreased the networks moduli much quicker than a like amount of B_1 added to networks prepared from lower molecular weight precursors. In this case, trapped entanglements are released in both networks, but since entanglements contribute more to the modulus of high molecular weight networks, a more noticeable effect was observed on their modulus.

The swelling results of the networks using the Flory-Rehner model are consistent with their mechanical properties. The model networks swelled less than predicted by the affine and phantom models, and their values of υ_2 showed no indication of decreasing to zero with decreasing density of elastic chains, ν. The swelling of the imperfect networks exhibited a stronger dependence on ν than the model networks and fall to approximately zero as ν decreases.

The swelling results can be adequately predicted over a wide range of swelling extents by the Flory-Rehner model if the phantom network model is assumed and the entanglements are experimentally accounted for by using the elastic moduli results for the values of the cycle rank, $(\nu - \mu)$. Using the above method, values of χ and their concentration dependence for PDMS in toluene and benzene were found to be in good agreement with literature values determined from solutions of uncrosslinked PDMS in the same solvents.

APPENDIX A.

The expressions given below are based on the Macosko-Miller model[29-31] and are used to calculate the structure parameters of the networks in this work. $M_{n,el}$, the number average molecular weight of the elastic chains is given by

$$M_{n,el} = 2\,M_A + \frac{M_{n,B_2} + (M_{A_4} - 2\,M_A)\,C}{(1-C)} \qquad (A.1)$$

where M_4 is the molecular weight of one arm of an A_4 unit, M_{A_4} is the molecular weight of A_4, and C is

$$C = \frac{3\,(1-\alpha)\,\alpha^2}{3\,(1-\alpha)\,\alpha^2 + 3\,(1-\alpha)^2\,\alpha + 3\,(1-\alpha)^3} \qquad (A.2)$$

α is defined as the probability that if one picks up a silane group (A group) at random and looks out away from the parent molecule, all paths are finite. The term β is defined in the same manner, but for vinyl groups. The terms α and β are expressed as

$$\alpha = \sqrt{\frac{4 - 3\,r\,p^2\,b_2}{4\,r\,p^2\,b_2}} - \frac{1}{2} \qquad (A.3)$$

$$\beta = r\,p\left[\sqrt{\frac{4 - 3\,r\,p^2\,b_2}{4\,r\,p^2\,b_2}} - \frac{1}{2}\right]^3 + 1 - r\,p \qquad (A.4)$$

where r is the ratio of silane groups (A) to vinyl groups (B) in the

reaction mixture; p is the extent of reaction of A groups; and b_2 is the mole fraction of the vinyl groups and is given by

$$b_2 = \frac{2 B_2^0}{B_1^0 + 2 B_2^0} \tag{A.5}$$

where $B_1{}^0$ and $B_2{}^0$ are the number of moles of species B_1 and B_2 in the reactant mixture. The chain density, ν, and crosslink density, μ, are given by

$$\nu = \frac{A_4^0}{(1 - w_{sol})} [6 \alpha (1 - \alpha)^3 + 2 (1 - \alpha)^4] \tag{A.6}$$

and

$$\mu = \frac{A_4^0}{(1 - w_{sol})} [4 \alpha (1 - \alpha)^3 + (1 - \alpha)^4] \tag{A.7}$$

where $A_4{}^0$ is the number of moles of species A_4 and the soluble weight fraction is defined as

$$w_{sol} = w_{A_4} \alpha^4 + w_{B_2} \beta^2 + w_{B_1} \beta \tag{A.8}$$

Equations (A.8) and (A.5) in conjunction with Eqs. (A.3) and (A.4) are used to determine the extent of reaction p from w_{sol} since all other parameters are known from the composition of the initial reactant mixture. Once p is determined, the values of α, ν, μ, C, and $M_{n,el}$ can be readily calculated.

1.6 References

1. Wall, F.T. *J. Chem. Phys.*, 1943, 11, 527.

2. Flory, P.J. *Chem. Rev.*, 1944, 35, 51.

3. Flory, P.J. "*Principles of Polymer Chemistry*", Cornell University Press: Ithaca, NY 1953.

4. James, H.M.; Guth, E., *J. Chem Phys.*, 1943, 11, 455.

5. James, H.M.; Guth, E. *J. Chem Phys.*, 1947, 15, 669.

6. James, H.M.; Guth, E., *J. Polymer Sci.*, 1949, 4, 153.

7. Flory, P.J. *Proc. R. Soc. Lond. Ser. A*, 1976, 351, 351.

8. Flory, P.J. *J. Chem. Phys.* 1977, 66, 5720.

9. Erman, B.; Flory, P.J. *J. Chem Phys.*, 1978, 68, 5363.

10. Flory, P.J.; Erman, B. *Macromolecules*, 1982, 15, 800.

11. Edwards, S.F.; Vilgis T.A. *Rep Prog. Phys.*, 1988, 51, 243.

12. Ball, R.C.; Doi, M.; Edwards, S.F.; Warner, M. *Polymer*, 1981, 22, 1010.

13. Edwards, S.F.; Vilgis, T. *Polymer* ,1986, 27, 483.

14. Flory, P.J.; Rehner, J. *J. Chem Phys.*, 1943, 11, 521.

15. Flory, P.J. *J. Chem. Phys.*, 1942, 10, 51.

16. Huggins, M.L. *J. Am. Chem. Soc.*, 1942, 64, 1712.

17. Patel, S.K., PhD. Thesis, Cornell University, 1991.

18. Lee, C.L.; Frye, C.L.; Johannson, O.K. *Polymer Preprints*, 1969, 10, 1361.

19. Lee, C.L.; Johannson, O.K. *J. Poly. Sci.: Poly. Chem. Ed.*, 1976, 14, 729.

20. Lee, C.L.; Marko, O.W.; Johannson, O.K. *J. Poly. Sci.: Poly. Chem. Ed.*, 1976, 14, 743.

21. Lee, C.L. U.S. Patent #3,445,426 (1969).

22. Frye, C.L. U.S. Patent #3,360,525 (1967).

23. Lapp, A.; Herz, J.; Strazielle, C. *Makromol. Chem.*, 1985, 186, 1919.

24. Llorente. M.A.; Mark, J.E. *Macromolecules,* 1980, 13, 681.

25. Valles, E.M.; Macosko, C.W. *Macromolecules*, 1979, 12, 521.

26. Meyers, K.O.; Bye, M.L., Merrill, E.W. *Macromolecules*, 1980, 13, 1045.

27. Ferry, J.D., "*Viscoelastic Properties of Polymers*", 3rd ed., Wiley, New York (1980).

28. Weiss, P.; Herz, J.; Rempp P. *Makromol. Chem.*, 1970, 135, 249.

29. Macosko, C.W.; Miller, D.R. *Macromolecules*, 1976, 9, 199.

30. Miller, D.R.; Macosko, C.W. *Macromolecules*, 1976, 9, 206.

31. Miller, D.R.; Valles, E.M.; Macosko, C.W. *Polym Eng. and Sci.*, 1979, 19, 272.

32. Plazek, D.J.; Dannhauser, W.; Ferry, J.D. *J. Colloid Sci.*, 1979, 19,
272.

33. Valles, E.M.; Macosko, C.W. *Macromolecules*, 1979, 12, 673.

34. Opperman W.; Rennar, N. *Progr. Colloid & Polym. Sci.*, 1987, 75, 49.

35. Kuwahara, N.; Okazawa, T.; Kaneko, M. *J. Polym. Sci.: Part C*, 1968, 543.

36. Flory, P.J.; Shih, H. *Macromolecules*, 1972, 5, 761.

37. De Gennes, P.G., "*Scaling Concepts in Polymer Physics*", Cornell University Press: Ithaca, NY (1979).

38. Villar, M.A.; Bibbo, M.A.; Valles, E.M. *J. Appl. Polym. Sci: Appl Polym. Symp.*, 1991, 49, 115.

39. Oeser, R.; Ewen, B.; Richter, D.; Farago, B. *Phys. Rev. Letters*, 1988, 60, 1041.

CHAPTER TWO
POLYMER/SOLVENT INTERACTION PARAMETER IN NETWORKS

2.1 Introduction and Background

In the previous chapter, dynamical mechanical experiments were performed on well-defined endlinked polydimethylsiloxane (PDMS) networks to test the affine and phantom elasticity models. For the range of molecular weights of the precursor chains studied, $2500 < M_n < 58000$, the equilibrium shear moduli, G_e, of the networks were clearly larger than those predicted by the affine model. For the model networks prepared with precursor chains with M_n larger than 20,000, the modulus was essentially constant and equal to the rubbery plateau modulus of high molecular weight PDMS melts. This was an indication that the contribution from the increasing number of trapped entanglements dominated over that from the chemical crosslinks. These model networks, as well as "imperfect" PDMS networks containing large amounts of pendant chains, were also swollen to equilibrium in both toluene and benzene. The swelling equilibrium of networks has been modelled by Flory and Rehner[1] assuming that the free energy of mixing and the free energy of elasticity terms are additive. The Flory[2] and Huggins[3] solution theory for polymer-solvent mixtures was used to determine the free energy of mixing term and is expected to be adequate at moderate to high polymer concentrations, but the choice of which theory to use for the free energy of elasticity has been widely debated. Oeser et al.[4] neutron-spin-echo experiments on the crosslink dynamics in tetrafunctional PDMS model networks confirmed that the

extent of crosslink fluctuations follows qualitatively the predictions of the phantom network model and results in chapter one also support the use of the phantom network model for the free energy of elasticity term. In the latter work, the experimental values of the modulus were employed in conjunction with the Flory-Rehner expression and the phantom network model to predict the swelling data of both model and imperfect PDMS networks. With the assumption of a phantom network, the Flory-Rehner model can be expressed quantitatively by the following expression

$$-\left[\frac{\ln(1-\upsilon_2)+\upsilon_2+\chi\upsilon_2^2}{v_1\upsilon_2^{1/3}}\right]=\frac{G_e}{RT} \qquad (1)$$

where υ_2 is the polymer volume fraction at equilibrium swelling, χ is the polymer/solvent interaction parameter, v_1 is the solvent molar volume, R is the gas constant, T is the absolute temperature, and G_e is the equilibrium shear modulus of the unswollen network. G_e/RT has replaced the $(\nu - \mu)$ term in the original Flory-Rehner equation, where ν is the number of moles of elastic chains per unit volume of the network and μ is the number of moles of junctions per unit volume of the network. Any effect of trapped entanglements on swelling is incorporated in Eq. (1) when the experimental value of the modulus is used. Eq. (1) can be rearranged to solve for χ and its dependence on υ_2, as given by

$$\chi = -\left[\frac{\frac{G_e}{RT} v_1 \upsilon_2^{1/3} + \ln(1-\upsilon_2) + \upsilon_2}{\upsilon_2^2}\right] \qquad (2)$$

In chapter one, values of the χ parameters and their concentration dependence from PDMS networks swollen in toluene and benzene using Eq. (2) compared reasonably well to literature values obtained on linear PDMS solutions[5,6]. However, the validity of the Flory-Rehner assumption of additivity of mixing and elastic free energies has been challenged by the work of Neuburger and Eichinger[7] on the basis of differential swelling measurements. Also, others[8] have proposed that χ may have a dependence on crosslink density in addition to a dependence on υ_2. Here, further evidence of the applicability of the Flory-Rehner assumption to PDMS networks is presented.

To show this, two additional solvents are chosen to obtain swelling equilibria with PDMS networks previously synthesized. These solvents are 2,3 - dimethylpentane (DMP) and 2,2,4 - trimethylpentane (TMP). The selection of these two solvents was guided by: 1) the interaction parameters of these solvents with PDMS are known to be fairly concentration-independent[9] allowing us to side-step the issue and possible complications that arise from a υ_2-dependent χ. Also, a comparison can be made between interaction parameters obtained from networks using Eq. (2) and interaction parameters obtained from linear PDMS solutions at infinite dilution by intrinsic viscosity, and (2) these are appreciably better solvents than benzene or toluene previously studied, and would lead to greater swelling of the networks. This

increased swelling may cause deviations from the Flory-Rehner theory in Eq. (1) due to possible excluded volume effects unaccounted for by the theory for high swelling ratios.

2.2 Experimental Methods

2.2.1 Characteristics of the PDMS Chains and Networks

The preparation of the PDMS precursor chains and networks were described in section 1.3. Tables 2.1 and 2.2 list the properties of the model and imperfect networks respectively including sol fraction, w_{sol}, equilibrium shear moduli, reported as G_e/RT and $G_e/[RT(1 - w_{sol})^{1/3}$, and equilibrium polymer volume fractions in DMP and TMP, υ_2^{DMP} and υ_2^{TMP}. The term x in Table 2.2 is the molar fraction of monofunctional precursor PDMS chains, B1, in the initial mixture before crosslinking. The moduli were measured as given in section 1.3.3 and have been obtained after the samples have cured in situ between the parallel plates of a Rheometrics System Four mechanical spectrometer. A correction to the measured modulus can be made by taking $G_e/(1 - w_{sol})^{1/3}$ as the modulus of the network after sol extraction as was done in chapter one. However, from Tables 2.1 and 2.2, it is seen that this correction is usually very small and affects the results only slightly as will be indicated later. The values of the equilibrium polymer volume fraction, υ_2, were determined using standard gravimetric procedures assuming additivity of volumes[10].

The linear PDMS samples used in the viscosity experiments are listed in Table 2.3. The molecular weights used in the calculations were

Table 2.1

Model Network Characteristics

sample	M_n[(a)] (g/mol)	$w_{sol} \times 10^2$	G_e/RT (mol/m^3)	$G_e/RT(1-w_{sol})^{1/3}$ (mol/m^3)	υ_2^{DMP}	υ_2^{TMP}
A-1	2,460	0.374	303	303	0.373	0.385
A-2	6,160	0.281	184	184	0.292	0.301
A-3a	8,350	0.450	149	149	0.253	0.262
A-3b	8,350	0.436	154	154	0.263	0.270
A-4	10,300	0.353	156	156	0.256	0.275
A-5	10,900	0.556	149	149	0.237	0.271
A-6	16,800	2.78	74.2	74.9	0.186	0.192
A-7a	18,500	0.259	130	130	0.228	0.235
A-7b	18,500	1.21	102	102	0.200	0.208
A-8a	19,800	0.254	107	107	0.221	0.226
A-8b	19,800	0.573	109	109	0.218	0.228
A-9	20,100	1.14	82.2	82.5	0.204	0.211
A-10	28,200	0.550	82.2	82.3	0.205	0.202
A-11	53,500	0.236	79.4	79.4	0.195	0.198
A-12	58,000	2.63	74.2	74.9	0.162	0.175

[(a)] Molecular weight of precursor before crosslinking

Table 2.2

Imperfect Network Characteristics

sample	x	$w_{sol} \times 10^2$	G_e/RT (mol/m^3)	$G_e/RT(1-w_{sol})^{1/3}$ (mol/m^3)	υ_2^{DMP}	υ_2^{TMP}
$M_{n,B2} = 20{,}100$; $M_{n,B1} = 19{,}800$						
B-2	0.051	2.52	66.2	66.7	0.187	0.205
B-3	0.146	4.36	57.3	58.2	0.178	0.150
B-4	0.296	7.74	36.0	36.9	0.154	0.165
B-5	0.445	11.8	29.0	30.2	0.132	0.136
B-6	0.596	18.9	17.0	18.2	0.105	0.113
$M_{n,B2} = 58{,}000$; $M_{n,B1} = 71{,}200$						
B'-1	0.170	6.98	35.6	36.5	0.135	0.139
B'-2	0.336	14.5	21.8	23.0	0.105	0.108
B'-3	0.482	27.8	11.8	13.2	0.069	0.072
B'-4	0.622	39.6	4.45	5.26	0.047	0.048

Table 2.3

Uncrosslinked PDMS Sample Characteristics

sample	M_w g/mol	d[1]	$[\eta]^{2,3\text{-DMP}}$ dl/g x 10^2	$[\eta]^{2,2,4\text{-TMP}}$ dl/g x 10^2
V1	7,180	1.17	6.3	5.6
V2	16,000	1.26	10.5	9.9
V3	20,200	1.20	13.0	11.7
V4	24,300	1.21	14.2	13.3
V5	39,300	1.12	21.2	18.8
V6	46,800	1.25	23.5	21.4
V7	58,300	1.16	28.0	24.8
V8	67,900	1.27	32.0	29.5

[1] polydispersity determined by GPC

the weight-average, M_w, and were determined by gel permeation chromatography (GPC). The solvents, 2,3-DMP (Aldrich Chem. Co. 99+%) and 2,2,4-TMP (Aldrich Chem. Co. 99+%) were filtered through 0.20 μm filter paper prior to using for viscosity measurements. Their densities at 25 °C are 0.6909 g/cm^3 for DMP and 0.687 g/cm^3 for the TMP corresponding to molar volumes of 145.0 cm^3/mol and 166.3 cm^3/mol respectively.

2.2.2 Intrinsic Viscosity

Viscosity measurements were carried out for all eight linear PDMS samples with an Ubbelohde-type viscometer in a water bath at 25 ± 0.1 °C. Flow times were measured to a precision of 0.1 sec. The density of the polymer solutions were used in the calculation of the concentration c, of the relative viscosity η_r and of the specific viscosity η_{sp}. The intrinsic viscosities [η], were determined by extrapolating the η_{sp}/c and $(\ln \eta_r)/c$ versus c plots to zero concentration as suggested by Huggins[3] and Kraemer[11] respectively. The two values do not differ by more than 2%.

2.3 Results and Discussion.

2.3.1 Equilibrium Swelling

In Figs. 2.1a and 2.1b, the values of χ obtained using Eq. (2) with the experimental values of G_e and υ_2 are plotted as a function of υ_2 for the PDMS networks swollen in DMP and TMP respectively at 25 °C. There is scatter in the data, but the figures qualitatively show that χ's for

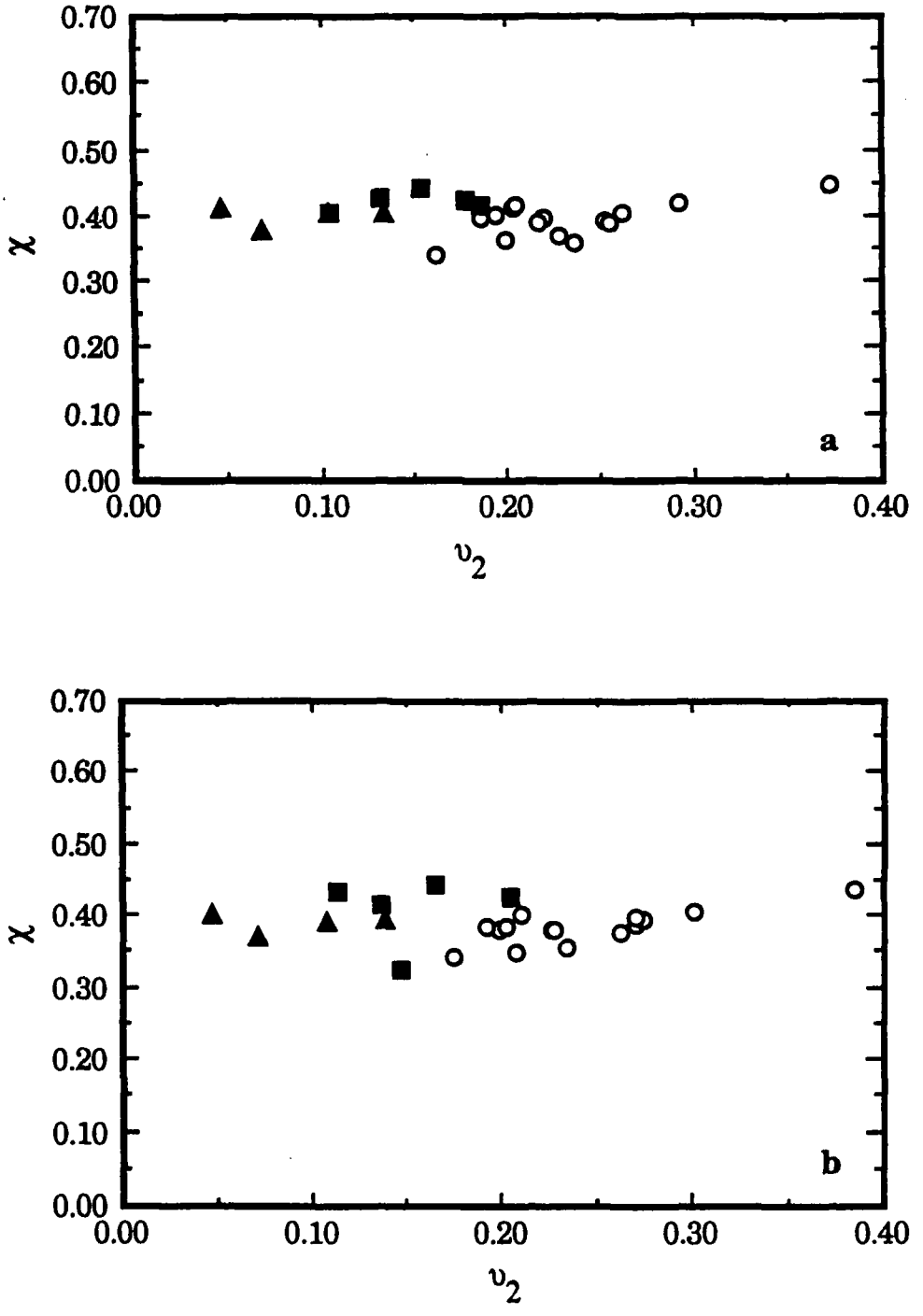

Figure 2.1. a) χ as a function of υ_2 for the networks swollen in 2,3-DMP where χ is calculated from the Flory-Rehner model (Eq. 2). The open symbols are for the model networks. The symbols ■ and ▲ are the data for the B and B' imperfect network series respectively from Table 2.2. b) same as in a) but for 2,2,4-TMP.

PDMS in DMP and TMP have very little υ_2 dependence as compared to benzene or toluene previously studied. It is suspected that the scatter in the data is primarily due to the accuracy in the modulus measurement as opposed to the measurement of υ_2 which was very reproducible. The very weak υ_2 dependence of χ for PDMS in DMP had previously been reported by Zhao and Eichinger[9], who used differential swelling experiments to determine χ for this system. They reported $\chi = 0.3485 + 0.0327\ \upsilon_2$. The data in Figs. 2.1a and 2.1b were fitted by a least-squares method to give $\chi = 0.392 \pm 0.025 + 0.038\ \upsilon_2$ for PDMS-DMP and $\chi = 0.380 \pm 0.030 + 0.045\ \upsilon_2$ for PDMS-TMP. When the value $G_e/[RT(1 - w_{sol})^{1/3}]$ is used in Eq. (2), only the χ values of the imperfect networks are affected (lowered by less than 10%) and therefore slightly lowering the intercept of the least squares fit to give, $\chi_0 = 0.385$ for PDMS-DMP and $\chi_0 = 0.365$ for PDMS-TMP. The dependence of χ on υ_2 increases when the modulus correction is used but the slope remains less than 0.1. This low υ_2 dependence is in contrast with those found for the same networks swollen in toluene and benzene, where the χ dependence on υ_2 was much greater (slope $\approx$ 0.3). The results indicate that TMP is a comparable or slightly better solvent than DMP at infinite dilution. However, for the range of υ_2's studied here, 0.047 to 0.385, DMP consistently swelled the networks to a slightly higher extent as shown in Tables 2.1 and 2.2 with the difference in swelling diminishing as lower values of υ_2 are approached. This is consistent with a slightly greater dependence of χ on υ_2 in TMP than in DMP.

2.3.2 Intrinsic Viscosity.

The value of χ in infinitely dilute systems can be obtained from intrinsic viscosity measurements. The method is based on the relationship originally developed by Stockmayer and Fixman[12] which allows the determination of χ for flexible chain polymers in any solvent from intrinsic viscosity and molecular weight values. Their equation is based on an expansion in terms of the square root of the molecular weight, $M^{1/2}$, and is thus limited to low and moderate molecular weights.[13] The relationship may be written as

$$\frac{[\eta]}{M^{1/2}} = K_\theta + 0.51\,\Phi_0 B M^{1/2} \qquad (4)$$

where K_θ is related to the unperturbed radius of gyration, $R_g^{\,o}$, of the polymer chain by

$$K_\theta = \Phi_0\, 6^{3/2} (R_g^{\,o})^3 M^{-3/2} \qquad (5)$$

and should be a constant independent of M and the solvent if draining effects are negligible[14].

The parameter B is related to the interaction parameter by

$$B = \frac{\upsilon_{sp}^2 (1 - 2\chi_0)}{v_1 N_A} \qquad (6)$$

where υ_{sp} is the specific volume of the polymer, v_1 is the solvent molar volume, N_A is Avogadro's number, χ_0 is the polymer/solvent interaction parameter at infinite polymer dilution, and Φ_0 is called the "universal" viscosity constant whose value will be discussed below.

For low dispersity polymer chains, M_w may be used for M in Eq (4). A plot of $[\eta]/M_w^{1/2}$ against $M_w^{1/2}$ should give a linear function whose intercept equals K_θ and slope is directly proportional to $(1-2\chi_0)$.

Examples of viscosity data for two of the linear PDMS samples examined, M_w = 20,200 and M_w = 67,900, are plotted in Fig. 2.2 in terms of η_{sp}/c and $\ln \eta_r/c$ versus c to show good convergence at c=0 yielding the value of $[\eta]$. Table 2.3 lists the values of $[\eta]$ determined for each polymer sample. The molecular weight and intrinsic viscosity data are used to determine the constants in the Mark-Houwink equation, $[\eta] = KM^a$, for the two systems studied here. Figures 2.3a and 2.3b are log-log plots showing the correlation between the intrinsic viscosity and the molecular weight giving a=0.728 and K= 9.50×10^{-5} for PDMS-DMP and a= 0.726 and K= 8.77×10^{-5} for PDMS-TMP. The constant a for each system is greater than 0.7 which indicates thermodynamically good solvents.

The Stockmayer-Fixman relationship is graphically shown in Figs. 2.4a and 2.4b for each solvent. As can be seen, a least-squares line fits the data quite well. The parameter B in Eq. (4) is related to the slope m of these curves by

$$B = m / (0.51\,\Phi_0) \qquad (7)$$

The interaction parameter χ_0 can then be obtained from Eqs. (5) and (7) as

$$\chi_0 = \frac{1}{2} - \frac{m v_1 N_A}{2.04 \upsilon_{sp}^2 \Phi_0} \qquad (8)$$

The value of χ_0 will depend on the value of Φ_0 chosen. Although called

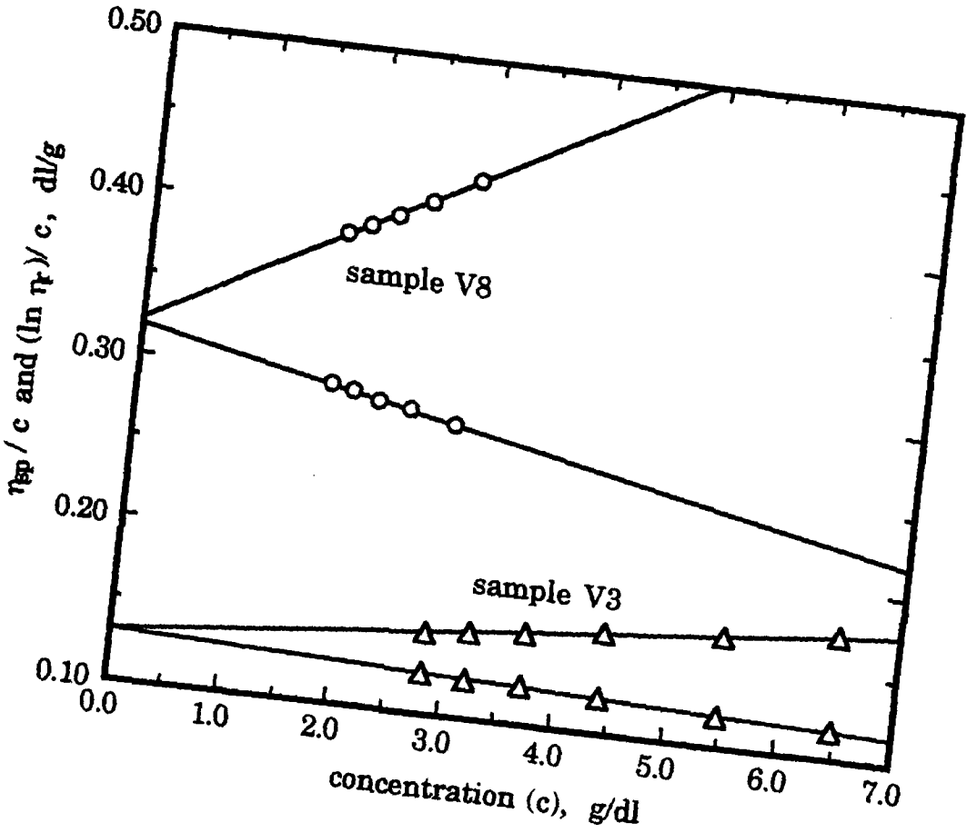

Figure 2.2. Huggins and Kraemer viscosity plots for samples V3 (M_w = 20200) and V8 (M_w = 67900) in 2,3-DMP at 25 °C.

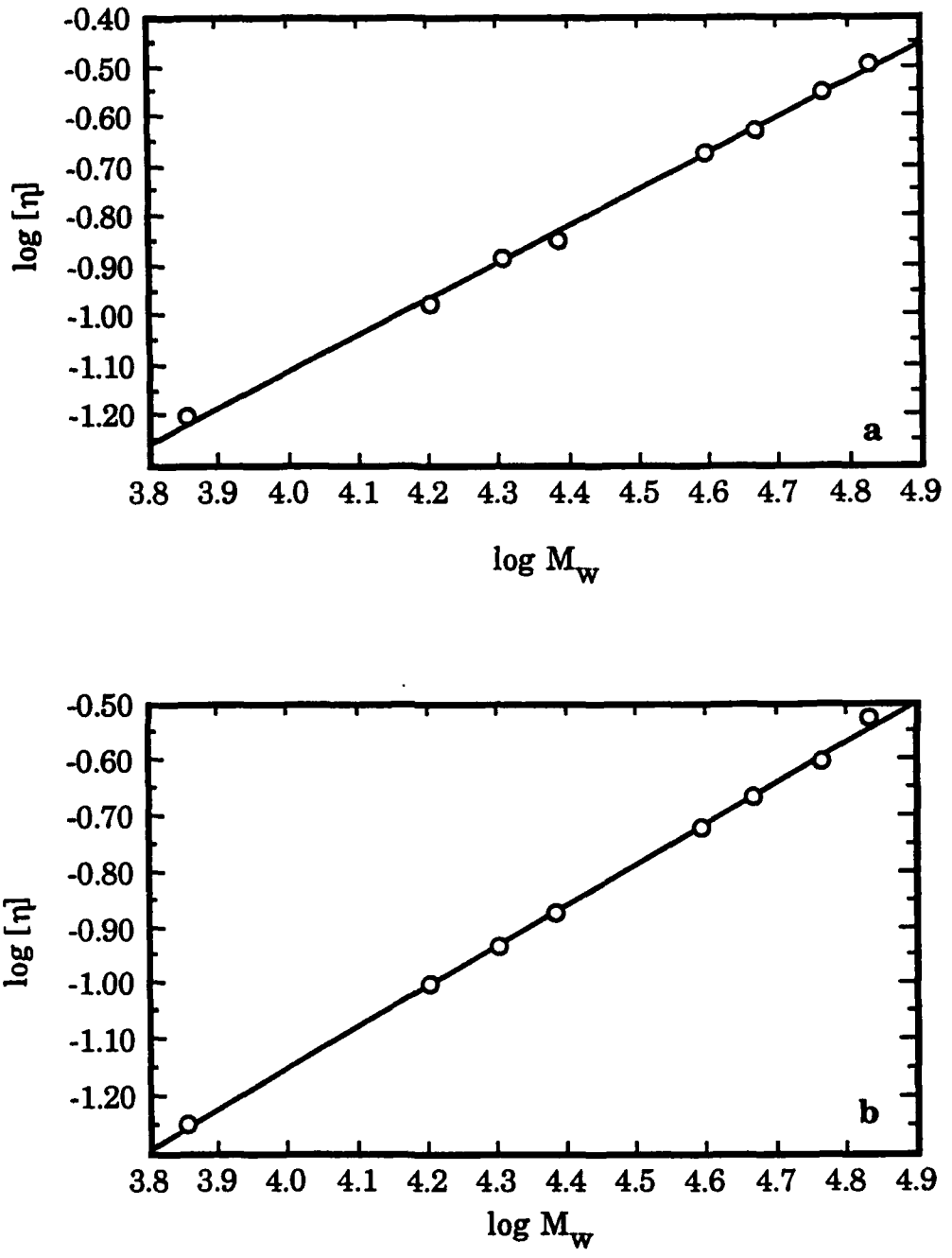

Figure 2.3. a) Log-log plot of [η] versus M_w for PDMS-DMP at 25 °C. b) same as in a) but for PDMS-TMP.

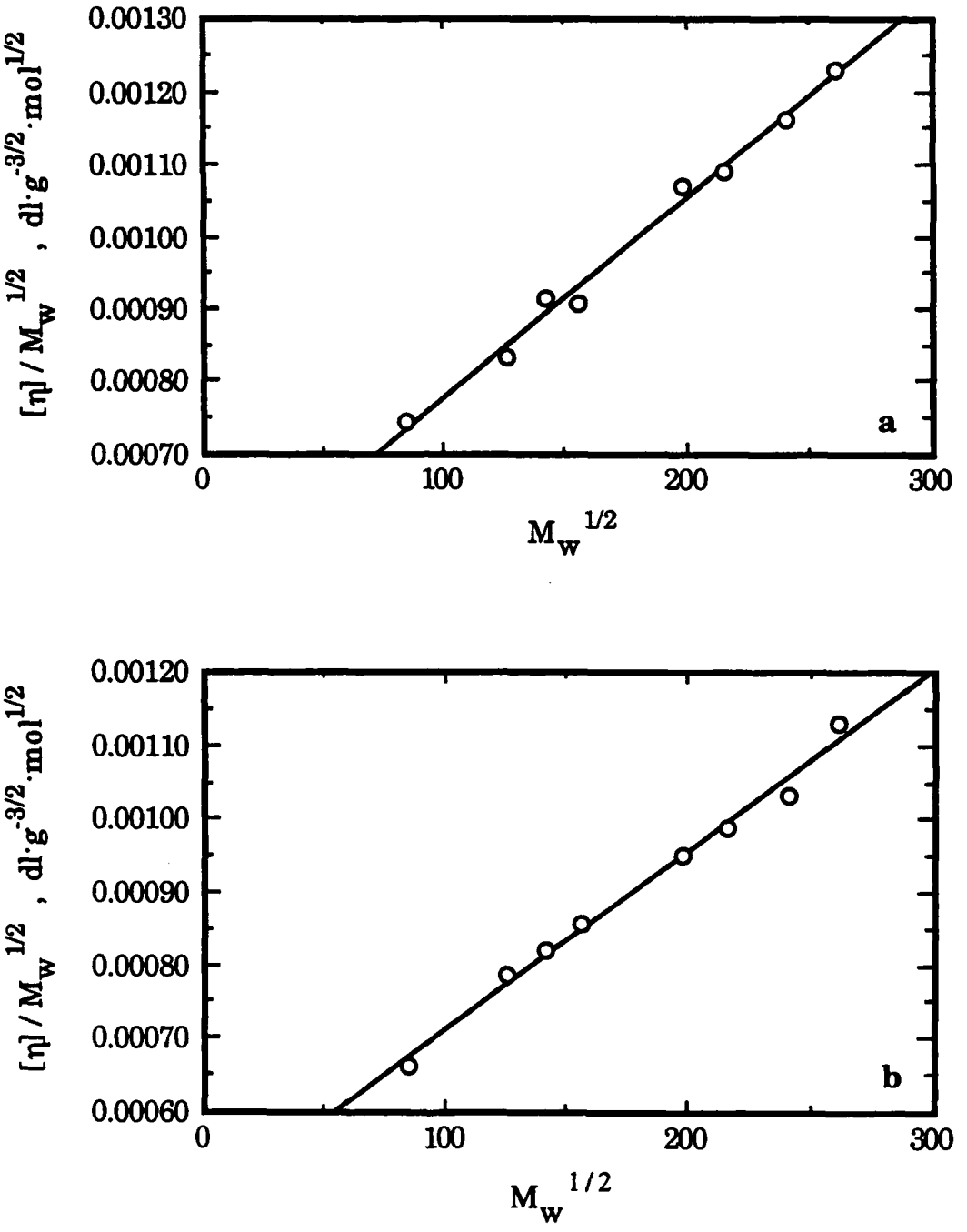

Figure 2.4. a) Stockmayer-Fixman relationship plotted as $[\eta]/M_w^{1/2}$ versus $M_w^{1/2}$ for the PDMS-DMP system. The slope of the best fit line is 2.77×10^{-6} dl·g^{-2}·mol$^{1/2}$ b) same as in a) but for PDMS-TMP. The slope of the best fit line is 2.50×10^{-6} dl·g^{-2}·mol$^{1/2}$.

a "universal" viscosity constant, Φ_0 has been shown to be dependent on the polymer/solvent system chosen[15-17] and for a polymer-solvent pair, Φ_0 may also depend on M_w[18]. Konishi et al.[18] used static and dynamic light scattering with viscosity measurements to determine Φ_0 for PDMS in bromocyclohexane at its theta temperature. For their range of molecular weights, 386,000 < M_w < 1,140,000, they observed that Φ_0 increased with M_w from 2.38 x 10^{23} mol^{-1} to 2.67 x 10^{23} mol^{-1}. They explain this observation as draining effects due to the hydrodynamically thin PDMS chains. Assuming this dependence of Φ_0 on M_w can be extended to lower molecular weight samples, then an extrapolation of the data of Konishi et al., using a log-log relationship between Φ_0 and M_w ,gives an approximate value of Φ_0 = 2.0 x 10^{23} mol^{-1} for the molecular weights studied here. This value of Φ_0 gives good agreement when used to calculate χ_0 from the intrinsic viscosity data of uncrosslinked PDMS chains in toluene, covering a similar range of molecular weights, from an earlier study[19]. The molecular weights of the PDMS chains from reference 19 were calculated from the viscosity data of the PDMS-toluene system using the Mark-Houwink parameters obtained by Lapp et al.[20] Using the Stockmayer-Fixman relation (Eq. 4) and a value of 2.0 x 10^{23} mol^{-1} for Φ_0, then the corresponding value of χ_0 for the PDMS-toluene system would be 0.440. This χ_0 value is within 1% of the value reported in the literature using osmometry[5] and within 3% of the value obtained from equilibrium swelling in chapter one.

For the molecular weight range of PDMS studied here, a value of Φ_0 = 2.0 x 10^{23} mol^{-1} is therefore a good approximation. Taking this

value of Φ_0 , the values of χ_0 for PDMS-DMP and PDMS-TMP can be extracted from the slopes of Figs 2.4a and 2.4b employing Eq. (8). The results give $\chi_0 = 0.388$ for PDMS-DMP and $\chi_0 = 0.385$ for PDMS-TMP. These values are within 1% and 2% of the values obtained from the equilibrium swelling experiments in DMP and TMP respectively. A comparison of the χ_0 values for toluene, DMP, and TMP are shown in Table 2.4. The values of K_θ for PDMS in all of the solvents (toluene, DMP, and TMP) are consistent with each other and lie in the range of .045 to .050 $mol \cdot g^{-3/2} \cdot ml$. This value is appreciably smaller than the value of .075 $mol \cdot g^{-3/2} \cdot ml$ reported by Lapp et al.[20] for PDMS chains in solution with toluene using Eq. (4). Two effects may have contributed to this higher value of K_θ. First is the applicability of the Stockmayer-Fixman relationship (Eq. 4) to the high molecular weights used in the previous study (up to $M_w \sim 625{,}000$), and second is the dependence of Φ_0 on M_w[18] which by Eq. (5) leads to a higher average value of K_θ for higher ranges of molecular weights. Both of these effects may have contributed to the curvature that is apparent in the data of Lapp et al. when plotted as $[\eta]/M^{1/2}$ versus $M^{1/2}$.

Because of the very weak dependence of χ on υ_2, the value of χ can, to a good approximation, be taken as a constant and Eq. (1) can now be tested using the values of χ_0 obtained from the viscosity experiments. Figs. 2.5a and 2.5b show how well the Flory-Rehrer model coupled with the phantom network assumption describes the swelling data of PDMS in DMP and TMP respectively using constant interaction parameters.

Table 2.4

Comparison of χ_0 values of PDMS in solvents

solvent	χ_0 (swell) [a]	χ_0 (visc)[b]
toluene [c]	0.452 ± 0.012	0.440
2,3-dimethylpentane	0.392 ± 0.025	0.388
2,2,4-trimethylpentane	0.380 ± 0.030	0.385

[a] determined by least-squares fit to χ versus υ_2 data.

[b] determined using $\Phi_0 = 2.0 \times 10^{23}$ mol^{-1}.

[c] data obtained from reference 19.

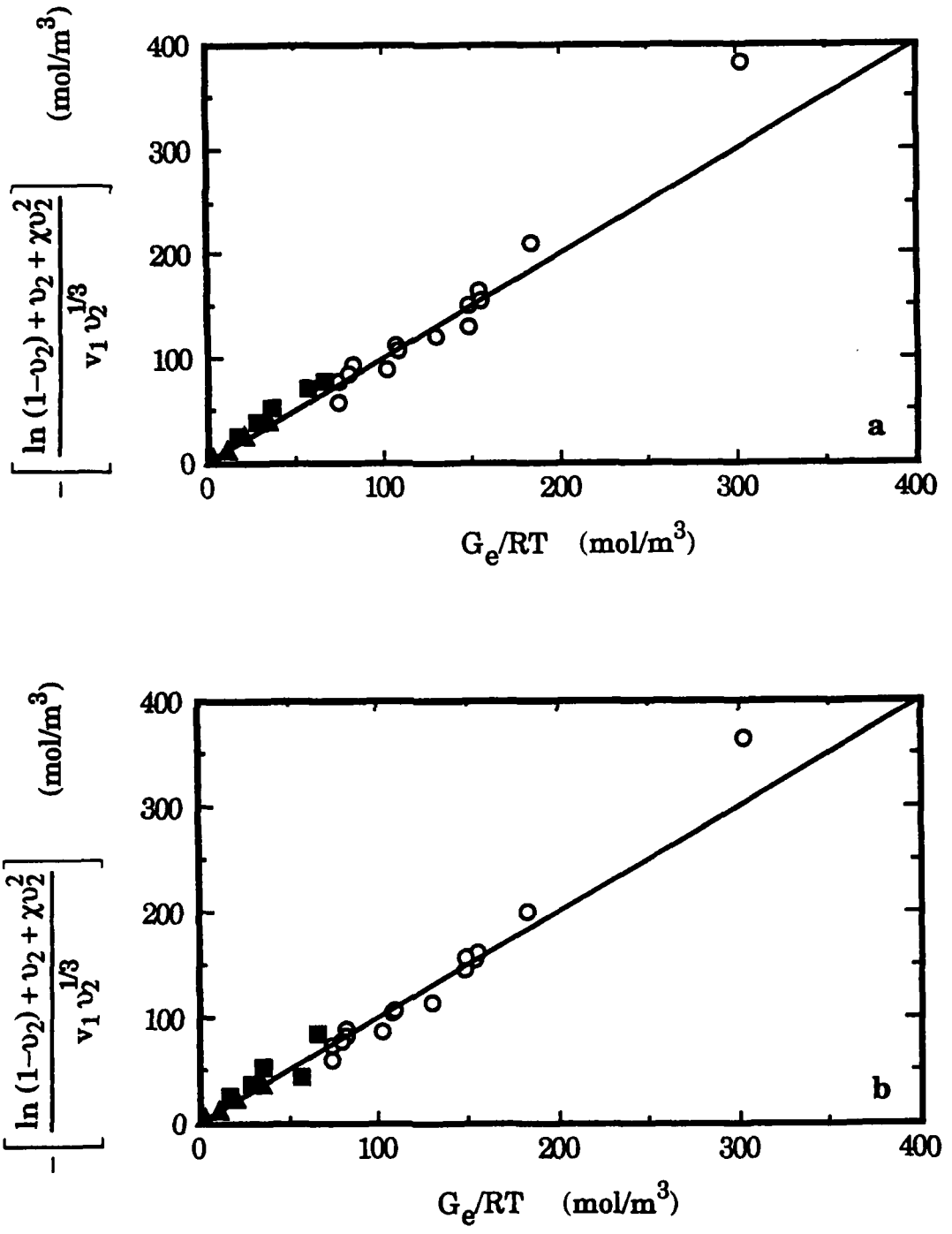

Figure 2.5. a) Comparison of swelling results of all networks swollen in 2,3-DMP using Eq. 1 and $\chi_0 = 0.388$. b) same as in a) but for 2,2,4-TMP and $\chi_0 = 0.385$. The symbols are the same as in Figure 2.1.

2.4 Conclusions.

Equilibrium swelling on well-defined model and imperfect PDMS networks were performed in two thermodynamically good solvents - 2,3-dimethylpentane and 2,2,4-trimethylpentane. By using the equilibrium shear moduli of the networks in the Flory-Rehner swelling model and assuming the phantom network, the polymer/solvent interaction parameter was determined as a function of polymer volume fraction. The χ values for the networks swollen in either solvent are virtually independent of polymer volume fraction.

Intrinsic viscosity measurements were used to find values for the interaction parameter at infinite dilution, χ_0, from uncrosslinked PDMS chains in solution with DMP and TMP through the use of the Stockmayer-Fixman relationship. It was found that the values of χ_0 agreed quite well with those determined from the equilibrium swelling experiments assuming a value of 2.0×10^{23} mol^{-1} for the universal viscosity constant in the molecular weight range $7{,}100 < M_w < 68{,}000$. Overall, it was found that for both solvents, the Flory-Rehner model coupled with the phantom network assumption adequately predicts the experimental swelling results when the experimental modulus and the interaction parameter determined from intrinsic viscosity are used.

With the solvents used in this work, the Flory-Rehner assumption was shown to hold for model and imperfect PDMS networks for solvents that are better than those previously used and that have an interaction parameter with PDMS that is essentially concentration

independent. Despite the better quality of DMP and TMP relative to benzene and toluene, the equilibrium volume fractions of the PDMS networks have remained quite high with the exception of four samples (see Table 2.2) that lead to $\upsilon_2 \leq 0.105$. Although one would expect excluded volume effects to start appearing in the semi-dilute regime[21], $\upsilon_2 < 0.1$, these effects must not be pronounced enough at the swelling values obtained here to show deviations from Flory-Rehner. Much higher swelling in gels have typically led to behavior consistent with the presence of excluded volume effects and the scaling laws of semi-dilute solutions[22-24]. The fact that the interaction parameter of the solvents used here is practically concentration independent and that the swelling can be described well with a constant χ indicate that no crosslink dependence on χ is necessary to describe the data presented here.

2.5 References

1. Flory, P.J.; Rehner, J. *J. Chem. Phys.* **1943**, 11, 521.

2. Flory, P.J. *J. Chem. Phys.* **1942**, 10, 51.

3. Huggins, M.L. *J. Am. Chem. Soc.* **1942**, 64, 1712.

4. Oeser, R.; Ewen, B.; Richter, D.; Farago, B. *Phys. Rev. Lett.* **1988**, 60, 1041.

5. Kuwahara, N.;Okazawa, T.; Kaneko, M. *J. Polym. Sci.: Part C* **1968**, 543.

6. Flory, P.J.; Shih, H. *Macromolecules* **1972**, 5, 761.

7. Neuburger, N.A.; Eichinger, B.E. *Macromolecules* **1988**, 21, 3060.

8. McKenna, G.B.; Flynn, K.M.; Chen, V. *Polymer Comm.* **1988**, 29, 272.

9. Zhao, Y.; Eichinger, B.E. *Polymer Preprints* **1991**, 32, 487.

10. Weiss, P.; Herz, J.; Rempp, P. *Makromol. Chem.* **1970**, 135, 249.

11. Kraemer, E.O. *Ind. Eng. Chem.* **1938**, 30, 1200.

12. Stockmayer, W.H.; Fixman, M. *J. Polym. Sci. : Part C* **1963**, 137.

13. Dondos, A.; Benoit, H. *Polymer* **1978**, 19, 523.

14. Flory, P.J. "Principles of Polymer Chemistry", Cornell University Press: Ithaca, NY, 1953.

15. Miyaki, Y.; Einaga, Y.; Fujita, H.; Fukuda, M. *Macromolecules* **1980**, 13, 588.

16. Berry, G.C. *J. Chem. Phys.* **1966**, 44, 4550.

17. Fukada, M.; Fukutomi, M.; Kato, Y.; Hashimoto, T. *J. Polym. Sci. : Polym. Phys. Ed.* **1974**, 12, 871.

18. Konishi, T.: Yoshizaki, T.; Yamakawa, H. *Macromolecules* **1991**, 24, 5614.

19. Patel, S.K. Ph.D. Thesis, Cornell University, **1991.**

20. Lapp, A.; Herz, J.; Strazielle, C. *Makromol. Chemie.* **1985**, 186, 1919.

21. De Gennes, P.G. *Scaling Concepts in Polymer Physics*, Cornell University Press: Ithaca, NY, **1979.**

22. Munch, J.P.; Candau S.; Herz, J.; Hild, G. *J. Physique* **1977**, 38, 971.

23. Bastide, J.; Picot C.; Candau S. *J. Polym. Sci. Polym. Phys. Ed.* **1979**, 17, 1441.

24. Horkay; Zrinyi *Macromolecules*, **1982**, 15, 1306.

CHAPTER THREE
SMALL ANGLE NEUTRON SCATTERING (SANS) OF INTERPENETRATING NETWORKS

3.1 Introduction and Background to SANS

Small angle neutron scattering (SANS) has become a very effective tool within the last decade in studying the physical properties of polymer systems such as single chain dimensions and polymer-polymer miscibility. Neutron scattering information is obtained by the method of isotope labeling and becomes advantageous since hydrogen (H) and deuterium (D) nuclei scatter neutrons differently due to their sizeable differences in mass and in coherent scattering lengths, but do not change the chemical structure of the polymer. Although blends of a polymer with its deuterated counterpart are expected to form ideal mixtures ($\chi = 0$), several workers[1-4] have measured small positive Flory-Huggins segment-segment interaction parameters, χ, in isotopic polymer mixtures using neutron scattering. This segment interaction leads to an upper critical solution temperature (UCST) and phase separation of the H-D polymer blend below this temperature.

Interpenetrating polymer networks (IPNs) are a type of polymer blend where at least one of the polymeric components is a network and are formed by either polymerizing a monomer within a network or crosslinking a polymer in the presence of another polymer or network[5]. Many IPNs phase separate upon formation of the network due to the loss of entropy of mixing between the network and polymer. Briber and Bauer[6] have shown from neutron scattering that IPNs of linear protonated polystyrene and cross-linked deuterated polystyrene

are homogeneous at low crosslink densities but phase separate when the crosslink density increases. Bauer et al.[7] observed similar behavior for compatible blends of linear poly(vinyl methyl ether) and crosslinked deuterated polystyrene. However, polystyrene-divinylbenzene networks are composed of divinylbenzene (DVB) nodules or clusters which give a wide distribution of crosslink densities[8]. These structures may affect the stability of an IPN synthesized from crosslinked polystyrene.

Polydimethylsiloxane (PDMS) networks that are endlinked give more uniform and better defined structures than those discussed above. Siloxane IPNs are formed either in the presence of nonfunctional PDMS chains that do not attach to the network or obtained by swelling endlinked networks with linear nonfunctional PDMS chains.

In this chapter, SANS measurements performed on two series of PDMS IPNs with different crosslink densities to study the effect of crosslink density on the network stability are presented. The first series of IPNs were prepared by endlinking difunctional PDMS (B_2), M_n = 53,500, in the presence of 25% by volume of mixtures of deuterated and protonated, nonfunctional (linear), PDMS chains. The linear polymer molecular weights were matched as closely as possible ($M_{n,H}$ = 13,200 and $M_{n,D}$ = 12,800). The second series of IPNs were synthesized using a B_2 precursor with a higher crosslink density (M_n = 10,900).

The first section of this chapter will describe the SANS theory applied to polymer blends and interpenetrating networks. The next

section will explain the experimental methods used to synthesize the deuterated PDMS chains, and the method of preparing the samples for neutron scattering. The last section will discuss the scattering of the IPNs, the effect of the crosslink density on the network's stability and the application of the Flory-Rehner model to polymer/polymer systems.

3.1.1 Polymer Blends

The neutron scattering intensity from a partially deuterated sample is directly proportional to the scattering structure factor S(q) where q is the scattering vector given by $(4\pi / \lambda)\sin\theta$ with λ being the wavelength of neutrons and θ the scattering angle. For a homogeneous binary polymer blend, de Gennes[9] obtained the following expression for S(q) based on a mean-field random phase approximation:

$$\frac{1}{S(q)} = [N_1 \phi_1 S_1(R_{g,1},q)]^{-1} + [N_2 \phi_2 S_2(R_{g,1},q)]^{-1} - 2\chi \qquad (1)$$

where N_i and ϕ_i, are the weight average degree of polymerization and volume fraction of polymer i (i = H or D), respectively. The term χ is the usual Flory-Huggins interaction parameter. Warner et. al[10] and others[11] have extended the de Gennes result to the case where the monomer volumes v_1 and v_2 of the components are not equal to get

$$\frac{k_n}{S(q)} = [N_1 v_1 \phi_1 S_1(R_{g,1},q)]^{-1} + [N_2 v_2 \phi_2 S_2(R_{g,2},q)]^{-1} - \frac{2\chi}{v_0} \qquad (2)$$

where v_0 is the molar volume of the reference unit cell. The constant k_n is called the contrast factor and is defined as

$$k_n = N_{av}\left(\frac{b_1}{v_1} - \frac{b_2}{v_2}\right)^2 \qquad (3)$$

with N_{av} being Avogadro's number and b_i being the scattering length per mole of monomer i. The term $S_i(R_{g,i},q)$ in Eq. (1) is the single-chain structure factor and is represented by the Debye function given as (the subscript i on R_g is dropped for simplicity):

$$S_i(R_g,q) = \frac{2(R_g^2q^2 + e^{-R_g^2q^2} - 1)}{R_g^4q^4} \quad . \qquad (4)$$

R_g is the radius of gyration of an ideal (Gaussian) coil, $R_g = a\,(N/6)^{1/2}$, where the parameter a is the segment length.

In the limit of q=0, $S_i(0) = 1$ and Eq. (2) reduces to:

$$\frac{k_n}{S(0)} = \frac{1}{N_1 v_1 \phi_1} + \frac{1}{N_2 v_2 \phi_2} - \frac{2\chi}{v_0} \quad . \qquad (5)$$

The right-hand side of Eq. (5) corresponds to the second derivative of the Flory-Huggins free energy of mixing of the polymer blend with respect to ϕ_1, $\partial^2(\Delta A/RT)/\partial\phi_1^2$. It is by definition, zero along the spinodal curve (limit of thermodynamic stability) such that χ_s (value of χ on the spinodal) is given by:

$$\frac{\chi_s}{v_0} = \frac{1}{2}\left[(\phi_1 N_1 v_1)^{-1} + (\phi_2 N_2 v_2)^{-1}\right] \quad . \qquad (6)$$

In the limit of $R_g q \ll 1$, Eq. (4) simplifies to:

$$S_i(R_g,q) \approx \left(1 - \frac{1}{3}R_g^2 q^2\right) = \left(1 - \frac{1}{18}a^2 N_i q^2\right) \quad . \tag{7}$$

Equation (2) can then be expanded and written as

$$\frac{k_n}{S(q)} = \frac{k_n}{S(0)} + \frac{a^2 q^2}{18\,\phi_1 v_1} + \frac{a^2 q^2}{18\,\phi_2 v_2} \quad . \tag{8}$$

For the H-D blend under consideration $v_1 = v_2 = v$, and now

$$\frac{k_n}{S(q)} = \frac{k_n}{S(0)}\left(1 + \frac{a^2 q^2\,(S(0)/k_n)}{18\,\phi_1\,\phi_2\,v}\right) \tag{9}$$

which can be rewritten in the Ornstein-Zernike form[9]:

$$S(q) = \frac{S(0)}{1 + q^2\varepsilon^2} \tag{10}$$

where

$$\varepsilon^2 = \frac{a^2(S(0)/k_n)}{18\,\phi_1\,\phi_2\,v} = \frac{a^2}{36\,\phi_1\,\phi_2\,(v/v_0)\,(\chi_s - \chi)} \tag{11}$$

It is noted that when $v_1 = v_2 = v_0$, Eqs. (6) and (11) reduce to de Gennes's result for a polymer blend.

According to Eq. (10), a plot of $S(q)^{-1}$ versus q^2 for small q's is linear with the intercept being equal to the zero-angle scattering intensity, S(0), which can be used in Eq. (5) to determine the value χ for the blend.

3.1.2 Interpenetrating Networks (IPNs)

A three component mixture can be made by dissolving linear chain H-D mixtures of the same molecular weight in a network of the same polymer. For this case, the scattering intensity, I(q) is given by[12-13]

$$I(q) = k_n (1-\phi) N_1 v_1 [x(1-x) S_s(q) + x^2 S_T(q)] \qquad (12)$$

where N_1 is the degree of polymerization of the linear chains, x is the volume fraction of linear chains that are labeled (D), $S_s(q)$ is the single chain scattering function of the linear polymer given by Eq. (4) and $S_T(q)$ is the total scattering function which is defined as $S_T = S_s(q) + NQ(q)$ where N is the total number of chains and Q(q) is the intermolecular scattering.

The single chain scattering, $S_s(q)$ for a D-linear chain in a network can be calculated experimentally from Eq. (12) by making IPNs that are identical except that they contain different amounts of deuterated polymer (different x values). An IPN with only deuterated chains (x=1) gives a scattering intensity that is a combination of both intramolecular scattering, $S_s(q)$, and intermolecular scattering, Q(q). The value of Q(q) is very difficult to evaluate, which leaves Eq. (12) for inadequate for interpreting the scattering data. For this case, a relationship is derived between S(0) and the free energy of the system to describe the scattering.

In Chapter one it was shown that the elastic free energy of a deformed network following the phantom network model of James and Guth[14] was

$$\frac{\Delta A_{el}}{RT} = \frac{\xi}{2}(\alpha_x^2 + \alpha_y^2 + \alpha_z^2 - 3) \qquad (13)$$

where ξ is the cycle rank, $\nu - \mu$, and represents the number of moles of elastic chains minus the number of moles of crosslinks. If the network was formed in a diluent and then swollen isotropically, $\alpha_i = (\phi_s/\phi)^{1/3}$, where ϕ is the network volume fraction and ϕ_s is the network volume fraction at which the network was formed[15]. For a network prepared from the bulk, $\phi_s = 1$. Substitution of α into Eq. (13) yields

$$\frac{\Delta A_{el}}{RT} = \frac{3}{2}\xi(\phi_s^{2/3}\phi^{-2/3} - 1) \qquad (14)$$

For the case of a polymer blend where one component is a network, the free energy of mixing is given by

$$\frac{\Delta A_m}{RT} = n_1 \ln(1-\phi) + \left(\frac{N_1 v_1}{v_0}\right)\chi n_1 \phi \qquad (15)$$

where n_1 is the number of moles of linear chains, ϕ is the volume fraction of the network, N_1 is the number of monomer units in the linear polymer chain, v_1 is the molar volume of the monomer unit of the linear chain, and v_0 is the molar volume of the reference cell. For a monomeric solvent molecule, $N_1 = 1$, and v_0 is taken to be v_1 and the result of Flory and Huggins is recovered for the free energy of mixing between a network and solvent. The difference in the chemical potential of the linear chains in the network with that of the pure linear chains is found by assuming additivity of free energies (Eqs. 14 and 15) and taking $\mu_1 - \mu_1^0 = \partial(\Delta A/RT)/\partial n_1$ where ΔA is the total free

energy of the system:

$$\mu_1 - \mu_1^o = \xi^* \phi_s^{2/3} \phi^{1/3} N_1 v_1 + \ln(1-\phi) + \phi + \left(\frac{N_1 v_1}{v_0}\right)\chi\phi^2 \qquad (16)$$

where ξ^* is the cycle rank per volume of dry network (V_0). If the network is swollen to equilibrium with the polymer chains, Eq. (16) is equal to zero which gives a relation similar to that found for the network swollen to equilibrium in a solvent.

As in the case of the polymer-polymer solution (see Eq. 5), the zero angle scattering in a swollen network is related to $\partial^2(\Delta A^*/RT)/\partial\phi^2$ where ΔA^* is the free energy per unit volume ($\Delta A/V$), obtained from Eqs. (14) and (15)[6,27]:

$$\frac{\Delta A^*}{RT} = \frac{(1-\phi)\ln(1-\phi)}{N_1 v_1} + \frac{\chi}{v_0}\phi(1-\phi) + \frac{3}{2}\xi^*(\phi_s^{2/3}\phi^{1/3} - \phi). \quad (17)$$

From which one gets,

$$\frac{\partial^2(\Delta A^*/RT)}{\partial\phi^2} = -\frac{\xi^*}{3}\phi_s^{2/3}\phi^{-5/3} + \frac{1}{(1-\phi)N_1 v_1} - \frac{2\chi}{v_0} = \frac{k_n}{S(0)} \qquad (18)$$

A form of Eq. (18) has been used to extract values of χ for IPNs from experimentaly obtained S(0)[6-7].

3.2 Experimental Methods

3.2.1 Synthesis of Deuterated Monomers

To prepare deuterated PDMS chains, it was necessary to synthesize

the deuterated monomer (D_3) from which these chains were prepared. The method used to synthesize the perdeuterated monomer hexamethylcyclotrisiloxane (D_3) is a modification of the one used by Beltzung et al.[18] Their method was chosen to increase the amount of octamethylcyclotetrasiloxane (D_4) formed. The starting material was perdeuterated methanol, obtained from Aldrich Chemical Co., whose degree of deuteration was 99.8%. The following synthesis involved five main steps.

The first step was the synthesis of perdeuterated methyl iodide using a classical method reported in the literature[19-20]. The reaction scheme is

$$3\,CD_3OD + 3/2\,I_2 + P \rightarrow 3\,CD_3I + D_3PO_3$$

The apparatus used for this reaction is shown in Figure 3.1. To prevent iodine crystals from clogging the stopcock, a piece of loose fitting glass wool was placed in the bottom of the cylindrical separatory funnel, and a widebored (4-5 mm) stopcock was used as a further precaution. The side-arm of the separatory funnel was wrapped with aluminum foil to ensure the alcoholic vapor passed from the flask to the funnel so that the iodine was dissolved with hot alcohol. One hundred and eighty grams (0.709 mol) of iodine were added to the separatory funnel while 15.3 grams (0.494 mol) of purified red phosphorus and 50.78 grams (1.408 mol) of perdeuterated methanol were added to the 250 ml round bottom reaction flask along with a magnetic stir bar. The contents of the flask were gradually heated to about 70 °C until the methyl alcohol passed through the side arm and

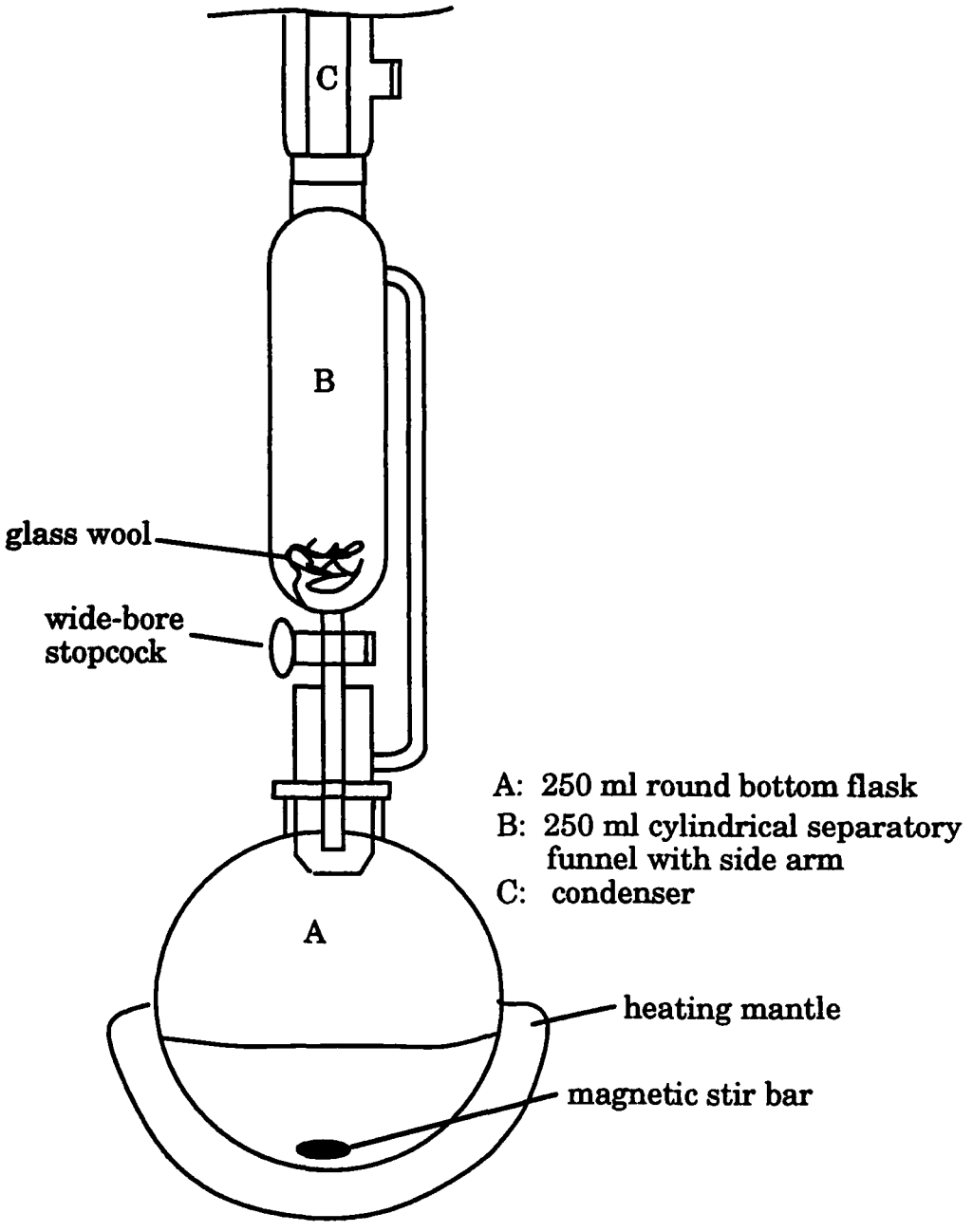

Figure 3.1. Apparatus used for the synthesis of methyl iodide

onto the iodine. After the iodine was wetted with the methanol, the stopcock was opened slightly to allow the iodine solution to drip into the reaction flask. After several minutes, enough methyl iodide was formed in the flask to start refluxing. The solution of iodine in the separatory funnel was added to the reaction flask at a controlled rate to allow a steady reflux. As more methyl iodide was formed, (which has a lower boiling point than methanol) the temperature was lowered to control the refluxing. After all the iodine had been dissolved and added to the reaction flask (2-3 hours), the contents were refluxed for an additional two hours. After the refluxing the stopcock was closed and the methyl iodide was distilled from the flask into the separatory funnel (b.p. 42 °C). The crude product was washed successively in 5% aqueous thiosulfate ($Na_2S_2O_3$) to remove any red color, water, 6N HCl to remove any unreacted alcohol if present[20], water, and 5% aqueous sodium bicarbonate ($NaHCO_3$). The iodide was dried with calcium chloride for 1 hour, filtered through glass wool, and then placed in a flask containing a short coil of copper wire. The iodide was stored in the dark until needed since it deteriorates rapidly when exposed to light[21]. The reaction gave a 77.0% yield (157g) of CD_3I.

The second step was the preparation of bis (trideuteriomethyl) diphenylsilane from a classical Grignard reaction[22] given by the following reactions,

$$CD_3I + Mg \dashrightarrow CD_3MgI$$

$$2\,CD_3MgI + (C_6H_5)_2SiCl_2 \dashrightarrow (CD_3)_2Si(C_6H_5)_2 + 2\,MgICl$$

Both reactions are carried out in diethyl ether (Et_2O) which was dried over molecular sieves and distilled. The apparatus used, shown in Figure 3.2, was flushed with argon, flame dried, evacuated with a vacuum pump and repurged with argon. This procedure was repeated three times to ensure all moisture in the apparatus was removed. Thirty-five grams of magnesium turnings were added to the reaction flask along with a magnetic stir bar and the system was flame dried again. After cooling, 65 ml of ether was added to the reaction vessel via the separatory funnel. A solution of 157 g (1.05 mol) of CD_3I mixed in 150 ml of ether was placed in the separatory funnel. Approximately 5 ml of the iodide solution was added to the reaction flask with no stirring. The reaction started within a few minutes, as indicated by bubbling, after which the iodide solution was added dropwise, with stirring, at a rate allowing the mixture to reflux gently. Once all the methyl iodide solution was added (~ 90 min), the mixture was heated to reflux for an additional hour.

After cooling, a solution of 133 g (0.525 mol) of diphenyldichlorosilane (99%) in 65 ml of ether was placed in the separatory funnel and added dropwise to the vigorously stirred Grignard reagent solution prepared above. The mixture was refluxed for an hour after complete addition. The final ethereal solution was hydrolyzed by transfer to a cooled flask containing a mixture of 120 ml 4N sulphuric acid and 750 g crushed ice. Care must be taken to prevent any excess magnesium turnings from going into the acid/water mixture. The ethereal layer was separated from the

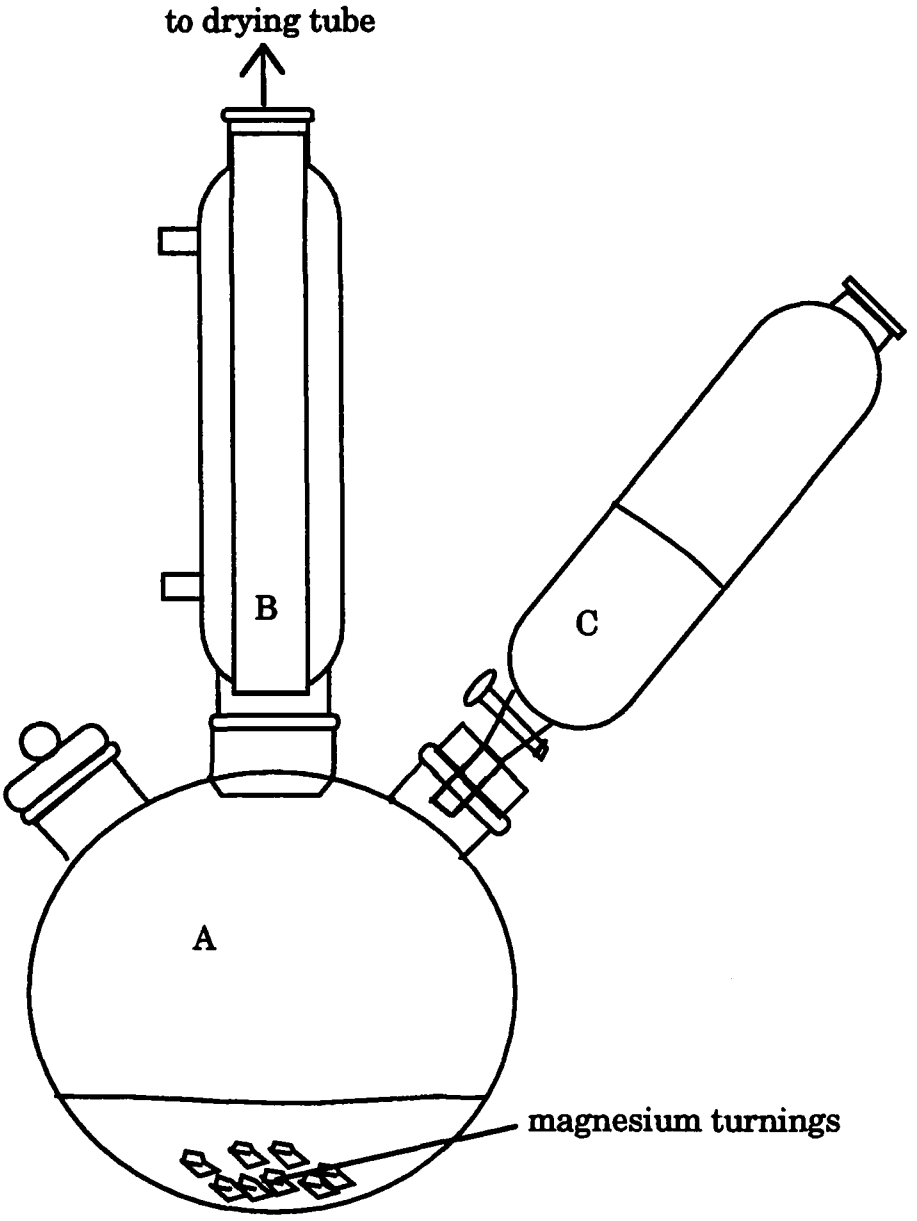

A: 1000 ml round bottom flask
B: condenser
C: 250 ml separatory funnel

Figure 3.2. Apparatus for Grignard Reaction

aqueous layer using a 500 ml separatory funnel. Any silane product present in the aqueous layer was extracted with three 100 ml portions of ether. The combined ethereal extracts were washed with 5% solutions of aqueous sodium thiosulfate and sodium bicarbonate successively, then dried with anhydrous calcium sulphate. The ether was evaporated off with a rota-evaporator and the remaining residue was vacuum distilled to obtain the silane product (b.p. 125 °C/ ~ 5 mm Hg). The yield of bis(trideuteriomethyl) diphenylsilane based on the initial quantity of CD_3I was 53.0% (61 g) with a degree of deuteration of 98.8% as determined by ^{H}NMR.

Step 3 involved the replacement of the phenyl groups of the previous product with chloro groups to obtain dimethyl dichlorosilane by the following reaction[18]

$$(CD_3)_2Si(C_6H_5)_2 + HCl \dashrightarrow (CD_3)_2SiCl_2 + 2\,C_6H_6$$

The reaction was performed in benzene with aluminum chloride ($AlCl_3$) as a catalyst. Using the apparatus in Figure 3.3, the system was flushed with argon and flame dried as done in the previous step. After cooling, a magnetic stir bar, 2 grams of $AlCl_3$ and 80 milliliters of benzene, previously dried on molecular sieves and distilled, were added to the reaction flask. The benzene solution was saturated with hydrogen chloride gas through the gas dispersion tube for 30 minutes. The flask was kept in a water bath maintained at 15 °C during the dropwise addition of $(CD_3)_2Si(C_6H_5)_2$. The HCl saturation was maintained during the reaction and 30 minutes after complete

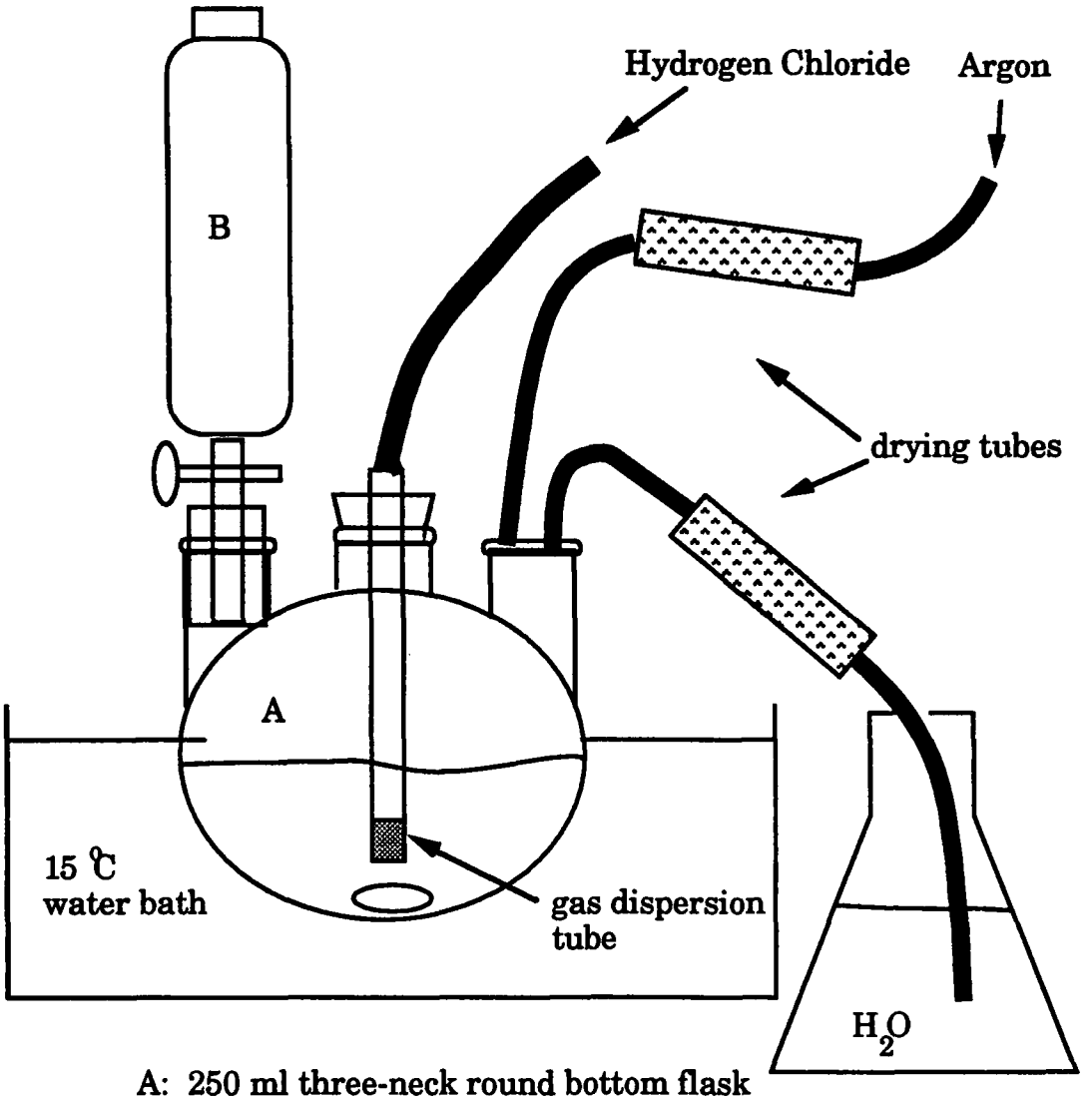

A: 250 ml three-neck round bottom flask
B: 250 ml separatory funnel

Figure 3.3 Apparatus setup for dimethyldichlorosilane synthesis

addition of the silane. A few milliliters of acetone were added to destroy the residual aluminum chloride and argon was purged through the system to evacuate excess HCl. The yellowish-orange product was distilled at 70-80 °C giving a clear mixture consisting of dimethyldichlorosilane and benzene.

The next step was the hydrolysis of the above chlorosilane which undergoes condensation to form mixtures of linear polysiloxanes and cyclosiloxanes[23] as shown by

$$(CD_3)_2SiCl_2 + 2H_2O \dashrightarrow (CD_3)_2Si(OH)_2 + 2HCl$$

$$m(CD_3)_2Si(OH)_2 \rightarrow \underset{\text{linear}}{HO\text{-}[Si(CD_3)_2]_x\text{-}OH} + \underset{\text{cyclics}}{[\,Si(CD_3)_2O]_n} + f(x,n)H_2O$$

where $x \geq 2$ and $n \geq 3$. The yield of cyclics was enhanced by using a water-miscible solvent (diethyl ether) and a strong acid medium (HCl). The hydrolysis was conducted by simultaneously adding the solution of the silane and distilled water from different separatory funnels at the same rate into a well stirred mixture of 40 ml of 7N HCl and 40 ml of ether. The temperature was kept at about 30 °C. The ethereal/benzene layer was separated from the aqueous layer and the solvents were carefully distilled off leaving 17g of an oily siloxane mixture.

The fifth and final step to obtain D_3 from the above mixture was the application of a thermal treatment known as cracking[23] using a base catalyst. The catalyst, KOH, allowed the rearrangement of the linear and cyclic siloxanes into the more favorable cyclotrisiloxane to occur at the lower temperature of 350 °C. Cracking at a reduced pressure

favors the formation of D_4. When a small amount of powdered KOH was added to the siloxane mixture and heated, D_3 that was present sublimed and formed crystals on the tube walls. The D_3 was collected during this process using the simple apparatus shown in Figure 3.4. After the crystals were collected off the tube walls, the mixture was reheated and more deuterated monomer was collected. In this preparation, 6.8 grams of D_3 crystals were collected over a period of 4 days.

The deuterated monomer was polymerized using the methods of section 1.3.1.

3.2.2 Preparation of IPNs for SANS

The molecular weight characteristics of the PDMS polymers used to synthesize the IPNs are listed in Table 3.1. The IPNs were formed by adding approximately 25% by volume of nonfunctional PDMS chains, referred to as linear chains, to pure difunctional PDMS precursors (B_2). The polydispersity of the chains, d, was determined by GPC. The volume fraction of linear PDMS that was deuterated varied from 0.25 to 1.0. The samples were mixed overnight on a slowly rotating turntable. After addition of the catalyst and mixing as discussed in section 1.3.2, the polymer mixtures were pipetted onto a 1/16 inch thick by 1 inch diameter cylindrical cell formed by a quartz disk, within an area defined by a 14 millimeter (inside diameter) by 1 millimeter thick rubber gasket which had been epoxied to the quartz disk. The samples were then covered with a second quartz disk to form a cell of uniform thickness and placed in an oven at 35 °C for three days to carry out the

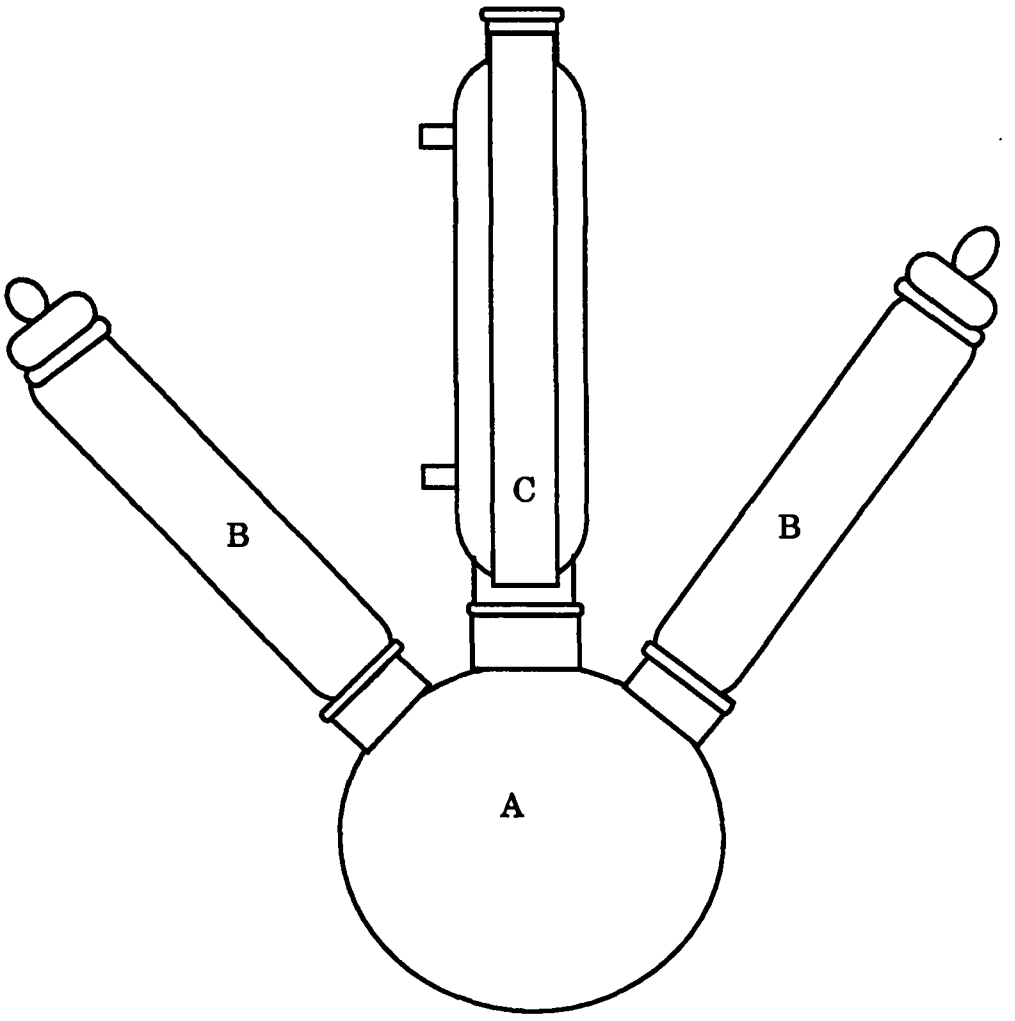

A: 200 ml three neck round bottom flask
B: collection tubes
C: condenser

Figure 3.4 Apparatus for collecting D_3 crystals

Table 3.1

Molecular Weight Characteristics of IPN Precursors

precursors	M_{n,B_2}	d	$M_{n,D}$ linear	d	$M_{n,H}$ linear	d
A[1]	-	-	12,800	1.35	13,700	1.23
E	53,500	1.27	12,800	1.35	13,200	1.23
G	10,900	1.19	12,800	1.35	13,200	1.23

[1] nonfunctional chains

endlinking reaction.

3.2.3 SANS Measurements

Small angle neutron scattering (SANS) measurements of the samples and calculations were performed by Barry Bauer and Robert Briber at the National Institute of Standards and Technology (NIST) 8 meter facility. The wavelength of the incoming neutron beam was 9 Angstrom with $\Delta\lambda/\lambda = 25$ % as determined by a rotating velocity selector. The scattering was done at 30 °C. The data was collected using a two dimensional detector and corrected for empty cell scattering and incoherent scattering. The scattered intensity was put on an absolute scale by using a secondary standard of silica gel.

3.3 Results and Discussion

3.3.1 Scattering of IPNs

Tables 3.1 and 3.2 list the characteristics of the PDMS H-D blends and IPNs that were studied in this work. Sample A-2 was a polymer blend with closely matched H and D molecular weights and can be used to calculate an interaction parameter from Eq. (2). IPNs in the E-series were formed from B_2 precursors with molecular weights much greater than the linear unattached chain molecular weight, whereas the G-series had B_2 precursors and unattached chains of approximately the same molecular weight. Each of the E and G series IPNs were prepared with approximately a constant 25% by volume of mixed H and D linear chains, but with the volume fraction of D chains

Table 3.2

Characteristics of Blends and IPNs

sample	ϕ (network)	x (D-linear)
A-2	0	0.261
E-1	0.756	1.0
E-2	0.735	0.720
E-3	0.754	0.471
E-4	0.698	0.225
G-1	0.758	1.0
G-2	0.758	0.716
G-3	0.759	0.472

(x) ranging from 0.25 to 1.0. Figures 3.5 and 3.6 are plots of the scattering from the E and G-series IPNs respectively. The lines through the points are fits of a single set of $S_s(q)$ and $S_T(q)$ determined from Eq. (12) for each data set in the series. This is accomplished by calculating the values $k_n(1-\phi)x(1-x)$ and $k_n(1-\phi)x^2$ for each sample in the E and G-series. The value of k_n was calculated using Eq. (3) and the scattering lengths of the atoms used[24]; -0.374 for H, 0.667 for D, 0.665 for C, 0.580 for O, and 0.441 for Si, with units of 10^{-12} cm. The molecular weight of the siloxane repeat unit $-Si(CH_3)_2O-$ is 74.15 and the density of PDMS is taken as 0.9697 g/cm^3 corresponding to a molar volume of the PDMS repeat unit as 76.4 cm^3/mol. The molar volume of the deuterated polymer was assumed to be the same as the protonated one. This gives a value of k_n = 0.00410 mol/cm^4. A problem arises since the values of ϕ are slightly different in each sample of a given series. Since the technique of extracting single chain data is rigorous only if the values of ϕ are identical, an approximation had to be made. In the E-1 sample, ϕ = 0.756 so it was assumed to be the same for all four samples in this series. This approximation is not very good for sample E-4 since its value of ϕ was 0.698. For this sample a deviation in the fit from the experimental data becomes apparent in Fig. 3.5. Figure 3.7 is a plot of the values of $S_s(q)$ used in the fits of the data in Figs. 3.5 and 3.6. The E-series was run on two separate occasions and both $S_s(q)$ data sets are shown in Fig. 3.7. The single chain scattering function is the one of present interest; the "total" scattering function is also obtained from the data in Figs. 3.5 and 3.6 using Eq. (12) but no conclusions are drawn from it. Because $S_s(q)$ is calculated as the

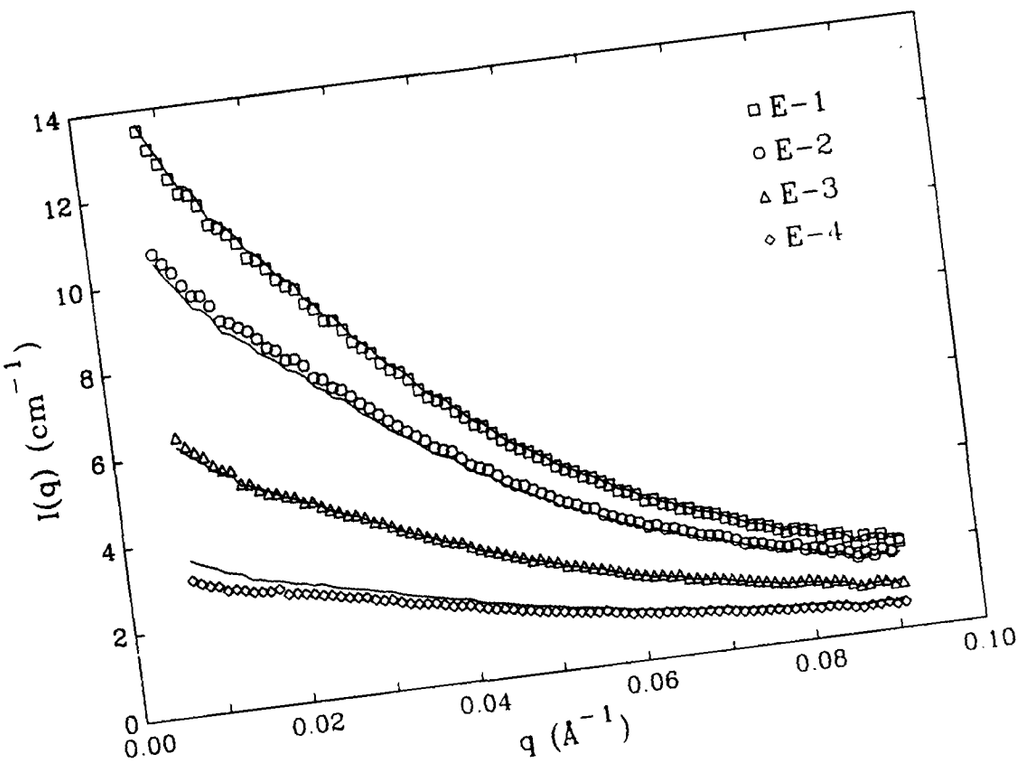

Fig. 3.5. Neutron scattering data of the interpenetrating networks of samples E-1 to E-4. The lines through the data represent a fit of a single set of $S_s(q)$ and $S_T(q)$ for the four data sets shown using Eq. (12).

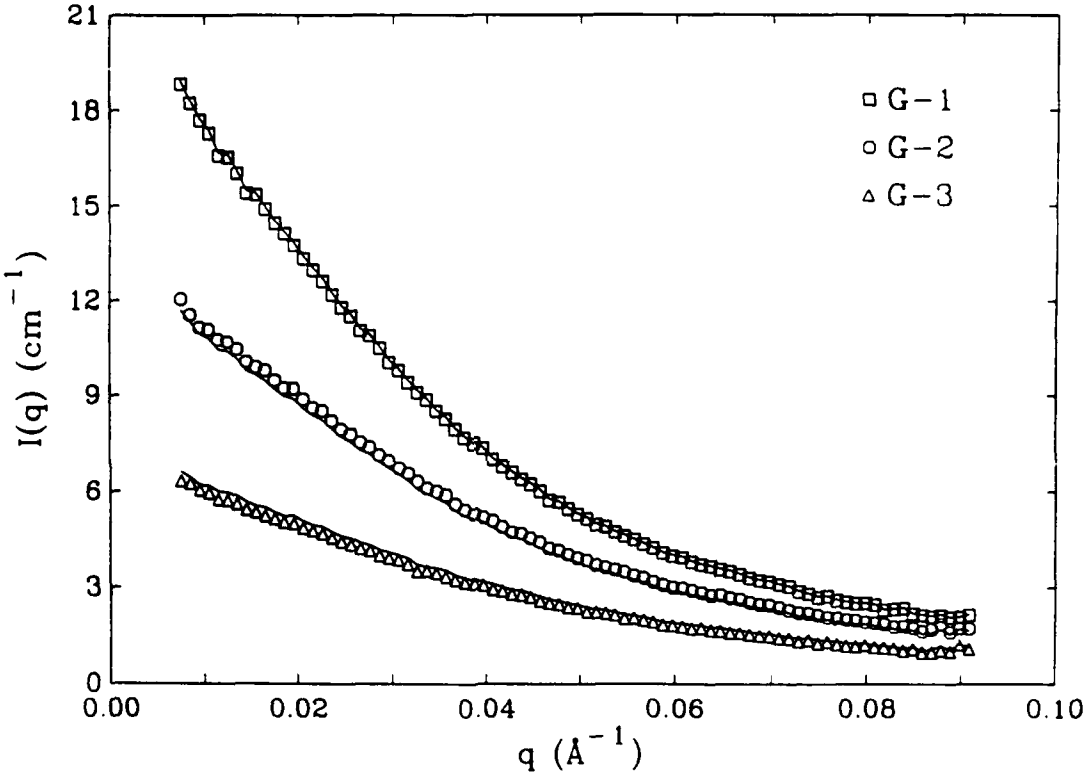

Fig. 3.6. Neutron scattering data of the interpenetrating networks of samples G-1 to G-3. The lines through the data represent a fit of a single set of $S_s(q)$ and $S_T(q)$ for the three data sets shown using Eq. (12).

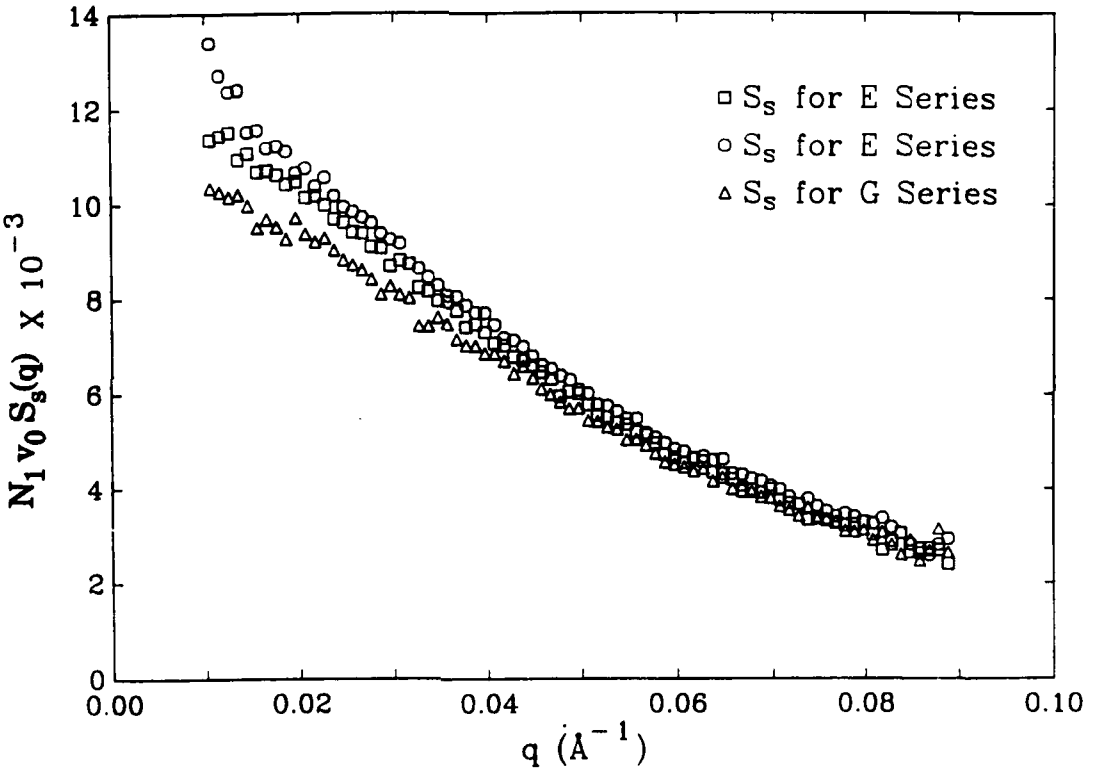

Fig. 3.7. Plot of the values of $S_s(q)$ used in the fits of the data in Figs. 3.5 and 3.6.

difference of data sets, there is noticeable scatter of the data points in Fig. 3.7. The calculated single chain scattering data of Fig. 3.7 at small q values is fitted with Eq. (7) to determine the radius of gyration (R_g) of the linear chains in the networks. Values of R_g for the three cases give 34.9, 37.3, and 32.2 Å giving an average R_g of 34.8 Å. This is reasonably close to the value of R_g = 37.5 Å calculated from the relation, $R_g = 0.285\ M_w^{1/2}$, obtained by Lapp et al.[25] using our GPC value of M_w = 17300 for the D linear chain. This is also consistent with a value of 33.1 Å calculated from Eq. (5) of chapter 2 from the viscosity results.

The average value of R_g obtained from the data in Fig 3.7 is used to calculate the interaction parameter χ for the blend A-2 using Eq. (2). A nonlinear least squares procedure[26] was used to fit Eq. (2) to the scattering data shown in Fig 3.8. The scattering experiments for the blend were done on two separate occasions and both are plotted in Fig. 3.8 showing the lines from the fitting of the data. The values of χ/v_0 calculated from the fits were 1.0×10^{-5} and 1.6×10^{-5} giving values of χ of 7.6×10^{-4} and 1.2×10^{-3} respectively where v_0 is taken as v_1. These values are slightly lower than but of the same order as the value of $\chi = 1.7 \times 10^{-3}$ reported by Lapp et al.[25] using H-D PDMS blends of different molecular weights. Samples E-1 and G-1, where x=1 (100% D-linear chains), are plotted in Fig. 3.9 and a comparison of the two samples indicates that there is more scattering intensity from the latter which contained a higher crosslink density than the former. This result is consistent with earlier results by Briber et al.[6] and Bauer et al.[7] on different IPN systems mentioned earlier. These workers utilize the Flory-Rehner model with the affine network assumption and an

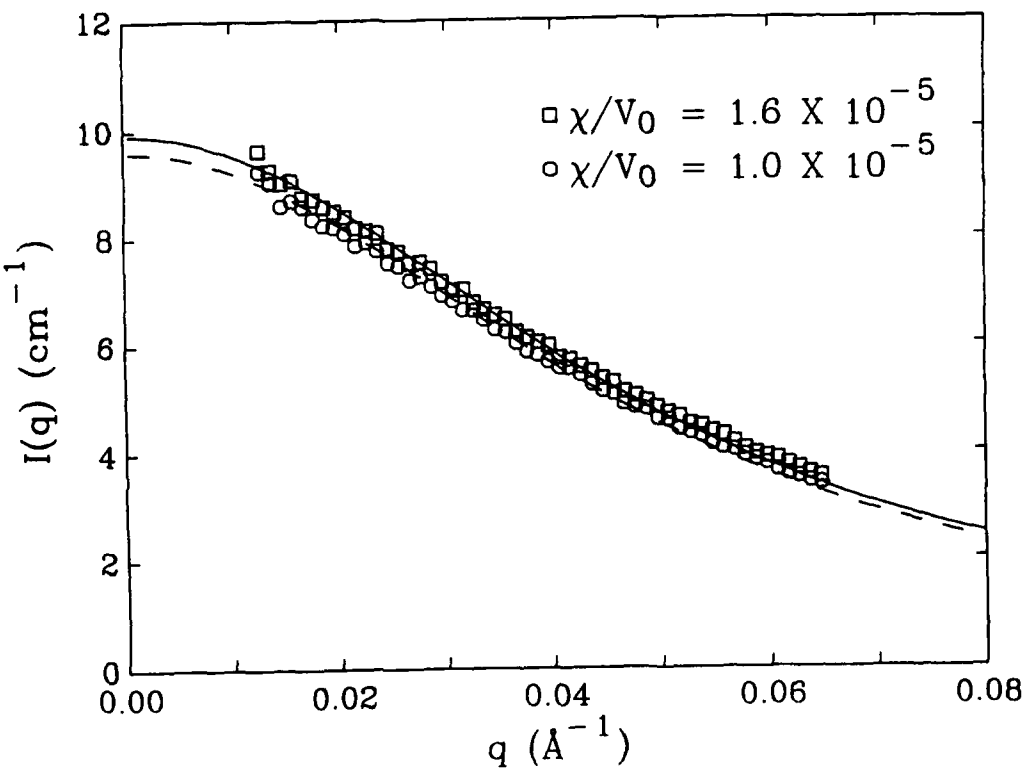

Fig. 3.8. Neutron scattering of blend A-2 done on two separate occasions. The lines are fits of the data using Eq. (2).

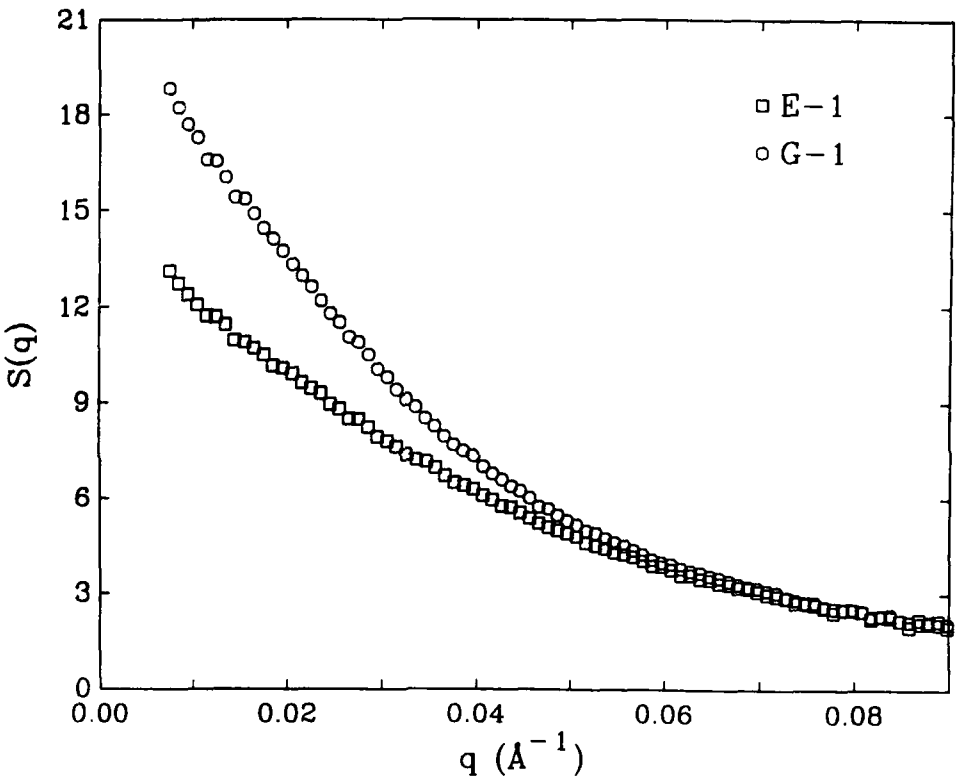

Fig. 3.9. Comparison of the scattering intensities of samples E-1 and G-1.

experimentally determined zero angle scattering intensity, S(0), for their IPNs to calculate an interaction parameter, χ, from Eq. (18) that is dependent on the number of elastic chains in the network. They find that χ increases as the crosslink density of their samples increases. Another explanation for the increase in scattering intensity is presented below.

3.3.2 Networks Swollen with Polymer Chains

Networks placed in polymer chains will absorb a given amount of those chains, analogous to networks swollen with a solvent. At equilibrium, the chemical potential of the linear chains in the network, given by Eq. (16), is equal to zero. The cycle rank, ξ^*, is replaced with G_e/RT as done in chapter one and $\chi = 0$ for mixing of like polymers to obtain:

$$-\left[\frac{\ln(1-\phi)+\phi}{N_1 v_1 \phi_s^{2/3} \phi^{1/3}}\right] = \frac{G_e}{RT} \qquad (20)$$

where G_e is the equilibrium modulus of the dry network, ϕ is the volume fraction of the swollen network, and v_1 is the molar volume of the linear chain monomer unit.

Some of the model and imperfect networks previously characterized in chapter one were allowed to swell to equilibrium with polymer chains of the same molecular weight (H-chains) as those used in the neutron scattering experiments. Table 3.3 lists the characteristics of the networks swollen with the polymer chains. The polymer chains used to swell the networks had a molecular weight of M_w = 16,200

Table 3.3

Characteristics of Networks Swollen with Chains

sample	G_e/RT (mol/m^3)	ϕ (in polymer chains)
C-1	184	0.880
C-2	154	0.838
C-3	149	0.839
C-4	130	0.821
C-5	79.4	0.692
C-6	36.0	0.660
C-7	21.8	0.500
C-8	17.0	0.492
C-9	11.8	0.383

(hence $N_1 = 219$). The swelling results are plotted as log ϕ versus log M_c in Fig 3.10, where the value M_c is the effective molecular weight between crosslinks as defined in chapter one. The value of v_1 was adjusted to 45.0 cm^3/mol in Eq. (20) to give the best fit curve to the experimental data in Fig 3.10. Although this value of v_1 is quite smaller than the theoretical value of 76.4 cm^3/mol, the molar volume of a large chain polymer molecule represented in the theory as N_1v_1 is not as easily defined as that of a solvent molecule. This becomes especially important when using the neutron scattering equations that contain the terms N_1v_1. At values of M_c less than 2,700 any swelling of the network with our polymer chains ($M_w \approx 16{,}000$) can no longer be measured within experimental error based on the data of Fig. 3.10. The region above the equilibrium swelling curve denoted by Region B in Fig. 3.10, represents a one phase region of networks swollen with polymer chains. As more chains are absorbed by a given network (given M_c) in this region, its volume fraction ϕ moves down the graph vertically until it reaches the curve (cannot swell any further) and is at equilibrium with the polymer chains. The region below and to the left of the equilibrium curve, Region A, represents networks that cannot be at equilibrium (they contain more solvent - linear chains - than they can absorb). Such networks if prepared under these conditions will microphase separate or will exude some of the solvent (macrophase separate). Such situations have been studied extensively with low molecular weight solvents[15].

To determine where samples E-1 and G-1 lie on Fig. 3.10, their values of M_c must first be determined. To find these values, IPNs of

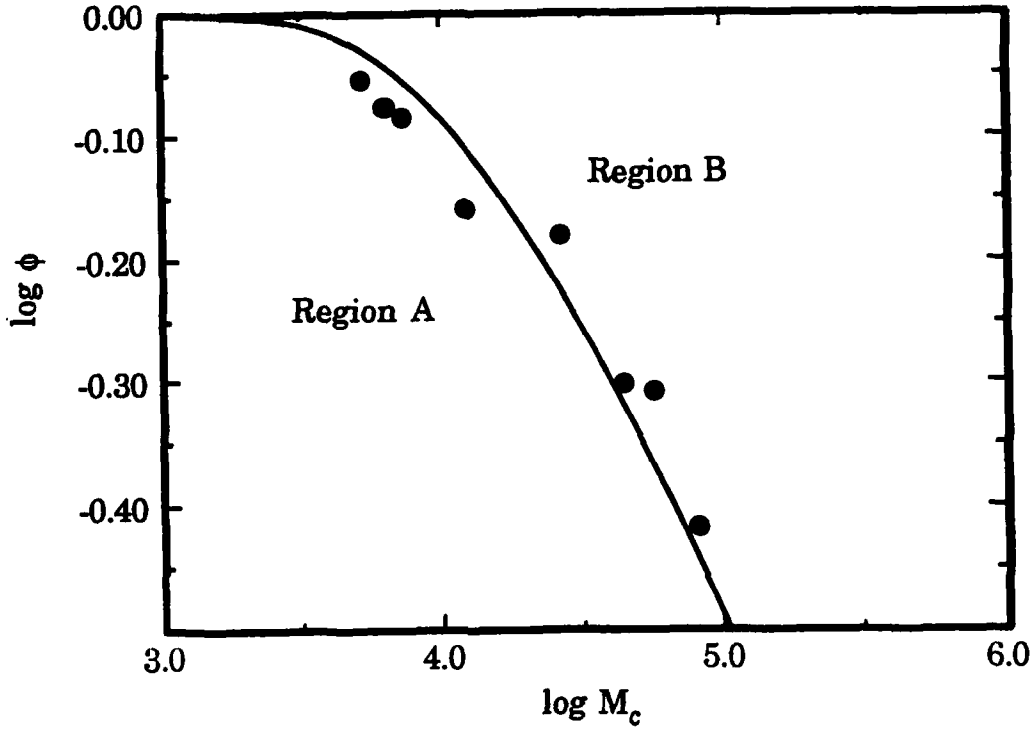

Fig. 3.10. Log-log plot giving the equilibrium swelling curve of networks swollen with polymer chains. The data points are from Table 3.3. The curve was constructed using Eq. (20). The value of N_1v_1 = 9,860 cm^3/mol was chosen to give the best fit to the experimental data.

identical molecular weight and volume fraction of linear polymer as in samples E-1 and G-1 were prepared (samples EE and GG of Table 3.4), except that only H-linear chains were used in the preparation. After the IPNs were formed, the linear polymer was extracted with toluene and then the network was swollen to equilibrium with toluene at 25 °C using the same procedures as in section 1.3.4. The equilibrium volume fraction, υ_2, of these networks in toluene were used to obtain a value of M_c from the correlation in Fig. 1.11. The values of υ_2 and M_c are listed in Table 3.4 for the two networks. To a good approximation, the values of M_c determined for samples EE and GG above can be used for samples E-1 and G-1 respectively. These values of M_c and the values of ϕ from Table 3.2 for the samples under consideration are plotted in Fig. 3.11 with the equilibrium swelling curve of Fig. 3.10. It can be seen that sample E-1 lies in the single phase region and sample G-1 lies slightly below the curve in the unstable region. Because of experimental error it cannot be said that sample G-1 is phase separated, but it does lie close enough to the curve to say that its network composition may cause significant scattering compared to that of sample E-1 which is farther from the equilibrium swelling curve and can absorb substantially more linear chains.

3.4 Conclusions

Two different series of interpenetrating networks (IPNs) were prepared for neutron scattering. One series of IPNs were prepared using B_2 precursors with a number average molecular weight, M_n of

Table 3.4

Values of M_c Extrapolated for E and G Samples

sample designation	υ_2 (in toluene)	M_c[1]
EE	0.191	22,900
GG	0.251	12,600

[1] extrapolated from Figure 1.11

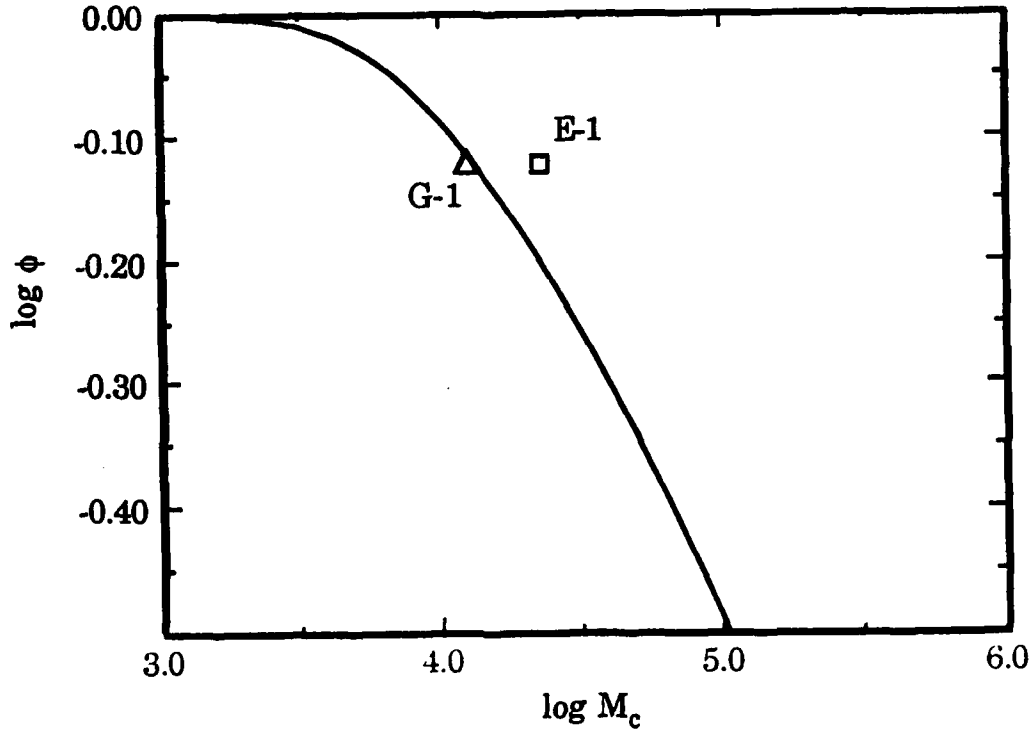

Fig. 3.11. Plot of log ϕ versus log M_c for samples E-1 and G-1 in relation to the equilibrium swelling curve from Fig. 3.10.

53,500, which was much greater than the M_n of the deuterated (D) linear unattached chains (Mn = 10,900). The other series of IPNs were prepared using B_2 precursors that were smaller in molecular weight than the linear chains. Single chain scattering of the D-chain was extracted by varying the volume fraction of D-chains within a series of constant chain volume fraction. From this extracted single chain scattering data, the radius of gyration, R_g for the chain can be determined. The average R_g of the three cases was 34.8 Å which was within experimental error of the value of 37.5 Å calculated from a relation determined by Lapp et al[25] and the value of 33.1 Å calculated from our viscosity data in chapter 2. The segment-segment interaction parameter, χ, of the H-D polymer blend of like molecular weights was obtained by using the average R_g value and employing a nonlinear least squares fit of Eq. (2) to the scattering data of the blend. For this work, an average χ for the H-D blend was calculated to be 1.0×10^{-3}.

For the same volume fraction of deuterated linear chains in networks of two different crosslink densities, the sample with the higher crosslink density gave a higher scattering intensity. This increased scattering was accounted for by where the samples lie in relation to the equilibrium swelling curve. This curve was constructed from the data of networks swollen with polymer chains of the same M_n as those in the neutron scattering experiments and applying the Flory-Rehner swelling model assuming the phantom network model. The molar volume of the polymer chain, N_1v_1, was adjusted to 9,860 cm^3/mol in the theoretical equation (Eq. 20) to fit the experimental data. It is not quite understood why the polymer chain had a smaller

molar volume than expected (16,700 cm^3/mol), but it is likely that dispersion of the polymer chains upon mixing with a network is a factor.

The effective molecular weight between crosslinks, M_c, was estimated for the samples used in the neutron scattering experiments by preparing similar IPNs in which the linear material was extracted and the networks swollen to equilibrium in toluene. Using the previously established correlation between υ_2 and M_c in chapter 1, a value for M_c in the samples used in neutron scattering was determined.

The IPN with the higher crosslink density was prepared under conditions in which it was very near the two-phase region of the equilibrium swelling curve whereas the lower crosslink density IPN was prepared such that it was clearly in the single phase region. The instability of the former led to neutron scattering that was much greater in intensity than the latter.

3.5 References

1. Bates, F.S.; Wignall, G.D.; Koehler, W.C. *Phys. Rev. Lett.*, 1985, 55, 2425.

2. Bates, F.S.; Dierker, S.B.; Wignall, G.D. *Macromolecules*, 1986, 19, 1938.

3. Yang, H.; Stein, R.S.; Han, C.C.; Bauer, B.J.; Kramer, E.J. *Polymer Communications*, 1986, 27, 132.

4. Bates, F.S.; Fetters, L.J.; Wignall, G.D. *Macromolecules*, 1988, 21, 1086.

5. Sperling, L.H. *"Interpenetrating Polymer Networks and Related Materials"*, Plenum Press: New York, 1981.

6. Briber, R.M.; Bauer, B.J. *Macromolecules*, 1991, 24, 1899.

7. Bauer, B.J.; Briber, R.M.; Han, C.C. *Macromolecules*, 1989, 22, 940.

8. Candau, S.; Bastide, J.; Delsanti, M. *Adv. Polym. Sci.*, 2982, 44, 27.

9. De Gennes, P.G. *"Scaling Concepts in Polymer Physics"*, Cornell University Press: Ithaca, NY, 1979.

10. Warner, M.; Higgins, J.S.; Carter, A.J. *Macromolecules*, 1983, 16, 1931.

11. Shibayama, M.; Yang, H.; Stein, R.S.; Han, C.C. *Macromolecules*, 1985, 18, 2179.

12. Benoit, H.; Koberstein, J.; Leibler, L. *Makromol. Chem. Suppl.*, 1981, 4, 85.

13. King, J.S.; Boyer, W.; Wignall, G.D., Ullman, R. *Macromolecules*, 1985, 18, 710.

14 James, H.; Guth, E. *J. Chem. Phys.*, 1947, 15, 669.

15. Dusek, K.; Prins, W. *Adv. Polym. Sci.*, 1969, 6, 1.

16. Flory, P.J. *J. Chem. Phys.*, 1942, 10, 51.

17. Huggins, M.L. *J. Am. Chem. Soc.*, 1942, 64, 1712.

18. Beltzung, M.; Picot, C.; Rempp, P.; Herz, J. *Macromolecules*, 1982, 15, 1594.

19. *"Organic Syntheses"*, Wiley: New York, 1950, Vol 2, p. 399.

20. Vogel, A.I. *"Practical Organic Chemistry"*, Wiley: New York, 1989, p. 287.

21. Perrin, D.D. *"Purification of Laboratory Chemicals"*, Pergamon Press: Oxford, 1988.

22. Vogel, A.I. *"Practical Organic Chemistry"*, Wiley: New York, 1989, p. 259.

23. Frisch, K.C. *"Cyclic Monomers"*, Wiley: New York, 1972.

24. Booth, C.*"Comprehensive Polymer Science"*, vol 1, Pergamon Press, New York (1989).

25. Lapp, A.; Picot, C.; Benoit, H. *Macromolecules*, 1985, 18, 2437.

26. Han, C.C; Bauer, B.J.; Clark, J.C.; Muroga, Y.; Matushita, Y.; Okada, M.; Tran-Cong, Q; Chang, T.; Sanchez, I.C. *Polymer*, 1988 29, 2002.

27. Brochard, F. *J. Physique*, 1981, 42, 505.